

CHAPTER 5

RESULTS AND DISCUSSIONS

5.1 Logistic Regression Model

5.1.1 Results and Validation

Data taken from Evans Country case study (Kleinbaum et al., 1982) was used to validate the logistic regression model developed using MATLAB. In the case study, the data was fitted to the logistic regression model using Java Script developed by Sullivan and Pezzullo (2007). Table 5.1 shows the comparison between the coefficients generated via Java Script codes and coefficients generated using MATLAB. The results showed that the logistic regression model developed in MATLAB produced the same coefficients as the results using Java Script by Kevin Sullivan. Thus, it is proved that the logistic regression model developed using MATLAB is acceptable.

Table 5.1: Comparison between coefficient using Java Script and MATLAB

Parameters	Results generated via Java Script (Sullivan & Pezzullo, 2007)	Results via developed model
Intercept	-2.9266	-2.9267
Variable 1 (catecholamine category)	1.3952	1.3953
Variable 2 (smoking category)	0.8653	0.8653
Variable 3 (interaction category)	-0.4498	-0.4498
Log-likelihood	417.8980	417.8980

5.1.2 Small Bore Results

The initial coefficients generated for small bore piping systems from MATLAB are shown in Table 5.2. It is observed that each of the coefficients are significant based on the p -value as it is lower than $\alpha = 0.05$ except for insulation type 1 (calcium silicate) which gave higher p -value. Thus, in this analysis, operating temperature showed a significant effect but insulation type gave no significance effect and may be removed from the model. Re-ran the analysis by excluding data on insulation type using the backward stepwise elimination method yields the following results as shown in Table 5.3.

Table 5.2: Initial coefficients generated for small bore piping systems

Parameter	Coefficient	Standard error	Wald test	p-value
Intercept	-4.1067	0.7491	-5.4822	0.0000
Age (year of service)	0.2365	0.0410	5.7683	0.0000
Temperature group				
Op. Temp G1	1.9212	0.4529	4.2420	0.0000
Op. Temp G2	1.7926	0.5634	3.1816	0.0015
Op. Temp G3	1.5733	0.5314	2.9607	0.0031
Op. Temp G4	1.6528	0.4482	3.6876	0.0000
Op. Temp G5	1.3735	0.5284	2.5994	0.0093
Type of insulation				
Insulation (calcium silicate)	0.1274	0.3775	0.3375	0.7357

Table 5.3: Final logistic regression model for small bore piping systems

Parameter	Coefficient	Standard error	Wald Test	p-value
Intercept	-3.9804	0.6461	-6.1610	0.0000
Age (year of service)	0.2366	0.0410	5.7701	0.0000
Temperature group				
Op. Temp G1	1.8954	0.4458	4.2515	0.0000
Op. Temp G2	1.6749	0.4404	3.8030	0.0001
Op. Temp G3	1.4695	0.4317	3.4038	0.0007
Op. Temp G4	1.6457	0.4473	3.6793	0.0002
Op. Temp G5	1.2761	0.4433	2.8785	0.0040

From Table 5.3, all p -values have shown significant values as the values were lower than $\alpha = 0.05$. Thus, a general equation of a linear function of independent variables for small bore piping systems can be written as

$$y(x) = -3.980 + 0.237x_1 + 1.895x_2 + 1.675x_3 + 1.470x_4 + 1.646x_5 + 1.276x_6 \quad (5.1)$$

where x_1 = pipe age (years in service); x_2, \dots, x_6 = dummy variable for operating temperature groups.

Eq. (5.1) can be further simplified where it will give different values for intercept for different operating temperature groups. For example, the new equation for pipe with operating temperature group 1 will be

$$y(x) = -3.980 + 0.237x_1 + 1.895(1) + 1.675(0) + 1.470(0) + 1.646(0) + 1.276(0) \quad (5.2)$$

by inserting $x_2 = 1$ and $x_3, \dots, x_6 = 0$. Solving Eq. (5.2), the simplified equation is

$$y(x) = -2.085 + 0.237x_1 \quad (5.3)$$

Table 5.4 shows the simplified equation for other groups of operating temperature by following the same step.

Table 5.4: The simplified equation for operating temperature group (small bore piping)

Operating temperature group	Description	Logistic Regression Model
Group 1	49°C to 93°C	$y(x) = -2.085 + 0.237x_1$
Group 2	-12°C to 16°C	$y(x) = -2.305 + 0.237x_1$
Group 3	16°C to 49°C	$y(x) = -2.511 + 0.237x_1$
Group 4	93°C to 121°C	$y(x) = -2.335 + 0.237x_1$
Group 5	Less than -12°C	$y(x) = -2.704 + 0.237x_1$
Group 6	More than 121°C	$y(x) = -3.980 + 0.237x_1$

Note: x_1 = age of pipes (years in service)

Let p_i be the probability of CUI occurrence in case i and the logistic regression model is (Hosmer & Lemeshow, 1989)

$$\text{logit}(p_i) = \log\left(\frac{p_i}{1-p_i}\right) = \beta_0 + \beta_1 x_1 \quad (5.4)$$

The logistic regression model presents the log odds of CUI occurrence as a linear function of pipe age with respect to operating temperature group. To predict the probability of CUI occurrence at certain years in service, the proposed model is Eq. (5.5) by rearranging Eq. (5.4).

$$p = \frac{e^{\beta_0 + \beta_1 x}}{1 + e^{\beta_0 + \beta_1 x}} \quad (5.5)$$

For example, using Eq. (5.3), the probability of CUI occurrence for the pipe after 10 years of service (age of pipe is 10 years old) is

$$p = \frac{e^{-2.085 + 0.237(10)}}{1 + e^{-2.085 + 0.237(10)}} = 0.570$$

This means after 10 years of pipe being in service, there is a 57% chance that the pipe will have CUI when the insulation is removed.

Sensitivity Analysis of Model

A sensitivity analysis was also performed to validate the proposed model. The logistic model was developed using two scenarios which are using 80% and 90% of the data set based on the proposed method by Ariaratnam et al. (2001). He proposed to randomly select 80% and 90% of the original data set and performed the logistic regression analysis accordingly. These two logistic models were subsequently compared to the proposed logistic model. The null and alternative hypotheses, H_0 and H_a , respectively, were tested for significance:

- H_0 : The models are equal (no significant difference between models).
- H_a : The models are different.

The three data sets are given in Table 5.6 and the coefficients generated by the three groups of data are given in Table 5.5. The results from Kruskal-Wallis test are given in Table 5.6.

Table 5.5: Coefficients for 100%, 90% and 80% of sample data (small bore piping)

Variable	100% of sample data		90% of sample data		80% of sample data	
	Estimate	p-value	Estimate	p-value	Estimate	p-value
Intercept	-3.9804	0.0000	-4.0380	0.0000	-4.0624	0.0000
Age	0.2366	0.0000	0.2334	0.0000	0.2419	0.0000
Op. Temp. 1	1.8954	0.0000	2.1649	0.0000	1.9004	0.0002
Op. Temp. 2	1.6749	0.0001	1.7502	0.0001	1.7586	0.0002
Op. Temp. 3	1.4695	0.0007	1.6522	0.0003	1.3076	0.0046
Op. Temp. 4	1.6457	0.0002	1.7561	0.0001	1.8386	0.0004
Op. Temp. 5	1.2761	0.0040	1.3631	0.0036	1.0156	0.0405

The sensitivity analysis revealed that $KW = 0.089$ compared with $\chi_{0.05,2}^2 = 5.991$. Therefore, the null hypothesis can be accepted, indicating that there is no significant difference among the three models. The proposed model seems to be a good representation of the observed data.

Table 5.6: Kruskal-Wallis Test for 100%, 90% and 80% of sample data (small bore piping)

Probability of occurrence			Rank Measure		
100%	90%	80%	100%	90%	80%
0.136	0.163	0.128	2	4	1
0.166	0.197	0.157	5	7	3
0.202	0.236	0.192	8	10	6
0.243	0.281	0.232	11	13	9
0.289	0.330	0.278	14	16	12
0.340	0.384	0.329	17	18	15
0.394	0.440	0.385	20	21	19
0.452	0.499	0.444	23	24	22
0.511	0.557	0.504	26	27	25
0.570	0.613	0.564	29	30	28
0.627	0.667	0.622	32	33	31
0.680	0.717	0.677	35	36	34
0.729	0.762	0.728	38	39	37
0.773	0.801	0.773	41	42	40
0.812	0.836	0.813	43	45	44
0.846	0.865	0.847	46	48	47
0.874	0.890	0.875	49	51	50
0.898	0.911	0.900	52	54	53
0.918	0.928	0.919	55	57	56
0.934	0.942	0.936	58	60	59
0.947	0.954	0.949	61	63	62
0.958	0.963	0.959	64	66	65
0.966	0.971	0.968	67	69	68
0.973	0.977	0.975	70	72	71
0.979	0.981	0.980	73	75	74
0.983	0.985	0.984	76	78	77
0.987	0.988	0.987	79	81	80
0.989	0.991	0.990	82	84	83
0.992	0.993	0.992	85	87	86
0.993	0.994	0.994	88	90	89
SUM:			1349	1400	1346
KW: 0.089			(KW = Kruskal-Wallis test statistic)		
$\chi^2_{0.05,2} = 5.991$					

5.1.3 Big Bore Results

The logistic model development for big bore piping system followed the same procedure as small bore. Table 5.7 provides initial coefficients from MATLAB software.

Table 5.7: Coefficients generated from MATLAB for big bore piping systems

Parameter	Coefficient	Standard error	Wald test	p-value
Intercept	-2.3992	0.2809	-8.5411	0.0000
Age (year of service)	0.1850	0.0163	11.3497	0.0000
Temperature group				
Op. Temp G1	0.5016	0.1626	3.0849	0.0020
Op. Temp G2	0.1093	0.1962	0.5571	0.5777
Op. Temp G3	0.2126	0.1702	1.2491	0.2116
Op. Temp G4	0.3720	0.1487	2.5017	0.0124
Op. Temp G5	-1.7991	0.3031	-5.9357	0.0000
Type of insulation				
Insulation (calcium silicate)	-0.8644	0.1179	-7.3316	0.0000

The results showed that the operating temperature and the insulation type are the significant variables based on the p -values as they were less than $\alpha = 0.05$ for big bore piping system. Note that the insulation type turns to be significant factor for big bore pipes. The simplified equation for each group of operating temperature is as shown in Table 5.8.

Table 5.8: Logistic regression models for big bore piping

Operating temperature group	Description	Insulation type	Logistic Regression Model
Group 1	49°C to 93°C	Calcium silicate	$y(x) = -2.762 + 0.185x_1$
Group 2	-12°C to 16°C	Calcium silicate	$y(x) = -3.154 + 0.185x_1$
Group 3	16°C to 49°C	Calcium silicate	$y(x) = -3.051 + 0.185x_1$
Group 4	93°C to 121°C	Calcium silicate	$y(x) = -2.892 + 0.185x_1$
Group 5	Less than -12°C	Calcium silicate	$y(x) = -5.063 + 0.185x_1$
Group 6	More than 121°C	Calcium silicate	$y(x) = -3.264 + 0.185x_1$
Group 1	49°C to 93°C	Cellular glass	$y(x) = -1.898 + 0.185x_1$
Group 2	-12°C to 16°C	Cellular glass	$y(x) = -2.290 + 0.185x_1$
Group 3	16°C to 49°C	Cellular glass	$y(x) = -2.187 + 0.185x_1$
Group 4	93°C to 121°C	Cellular glass	$y(x) = -2.027 + 0.185x_1$
Group 5	Less than -12°C	Cellular glass	$y(x) = -4.198 + 0.185x_1$
Group 6	More than 121°C	Cellular glass	$y(x) = -2.399 + 0.185x_1$

Note: x_1 = age of pipes (years in service)

Sensitivity Analysis of Model

A sensitivity analysis was also performed and followed the same steps taken as in the small bore analysis. 80% and 90% of the sample data and the results generated from these two models were subsequently compared to the original logistic model (100% sample data). The coefficients generated by the three sample data as shown in Table 5.10 are given in Table 5.9. The result from Kruskal- Wallis test is given in Table 5.10.

Table 5.9: Coefficients for 100%, 90% and 80% of sample data (big bore piping)

Variable	100% of sample data		90% of sample data		80% of sample data	
	Estimate	p-value	Estimate	p-value	Estimate	p-value
Intercept	-2.3992	0.0000	-2.3730	0.0000	-2.3898	0.0000
Age	0.1850	0.0000	0.1828	0.0000	0.1779	0.0000
Temp. 1	0.5016	0.0020	0.4143	0.0171	0.6199	0.0006
Temp. 2	0.1093	0.5777	0.1580	0.4454	0.1396	0.5237
Temp. 3	0.2126	0.2116	0.2452	0.1685	0.2258	0.2365
Temp. 4	0.3720	0.0124	0.3747	0.0165	0.5236	0.0015
Temp. 5	-1.7991	0.0000	-1.6754	0.0000	-1.6419	0.0000
Insulation type	-0.8644	0.0000	-0.8595	0.0000	-0.8555	0.0000

Table 5.10: Kruskal-Wallis Test for 100%, 90% and 80% of sample data (big bore piping)

Probability of occurrence			Rank Measure		
0.071	0.067	0.080	2	1	4
0.084	0.079	0.094	5	3	7
0.099	0.094	0.110	8	6	9
0.117	0.110	0.129	11	10	12
0.137	0.130	0.150	14	13	15
0.161	0.152	0.174	17	16	18
0.187	0.177	0.201	20	19	21
0.217	0.205	0.231	23	22	24
0.250	0.236	0.264	26	25	27
0.287	0.271	0.300	29	28	30
0.326	0.308	0.339	32	31	33
0.368	0.349	0.380	35	34	36
0.412	0.391	0.422	38	37	39
0.457	0.436	0.466	41	40	42
0.503	0.481	0.511	44	43	45
0.549	0.527	0.555	47	46	48
0.595	0.572	0.598	50	49	51
0.638	0.616	0.640	53	52	54
0.680	0.658	0.680	56	55	57
0.719	0.698	0.718	60	58	59
0.755	0.735	0.752	63	61	62
0.787	0.769	0.784	66	64	65
0.817	0.800	0.812	69	67	68
0.843	0.828	0.838	72	70	71
0.866	0.852	0.861	75	73	74
0.886	0.874	0.881	78	76	77
0.903	0.893	0.898	81	79	80
0.918	0.909	0.913	84	82	83
0.931	0.923	0.926	87	85	86
0.942	0.935	0.938	90	88	89
Sum			1376	1333	1386
$KW: 0.0775$ $\chi^2_{0.05,2} = 5.991$			(KW = Kruskal-Wallis test statistic)		

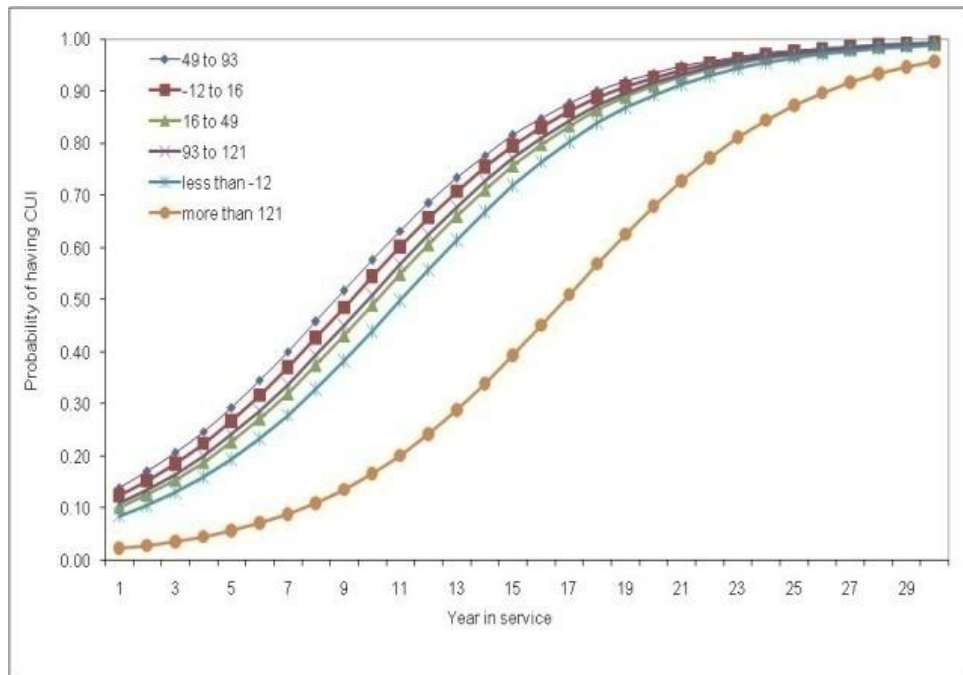
The sensitivity analysis has revealed that $KW = 0.077$ compared with $\chi^2_{0.05,2} = 5.991$. Therefore the null hypothesis may be accepted, indicating that there is no significant

different among the three models. The proposed model is a good representation of the observed data.

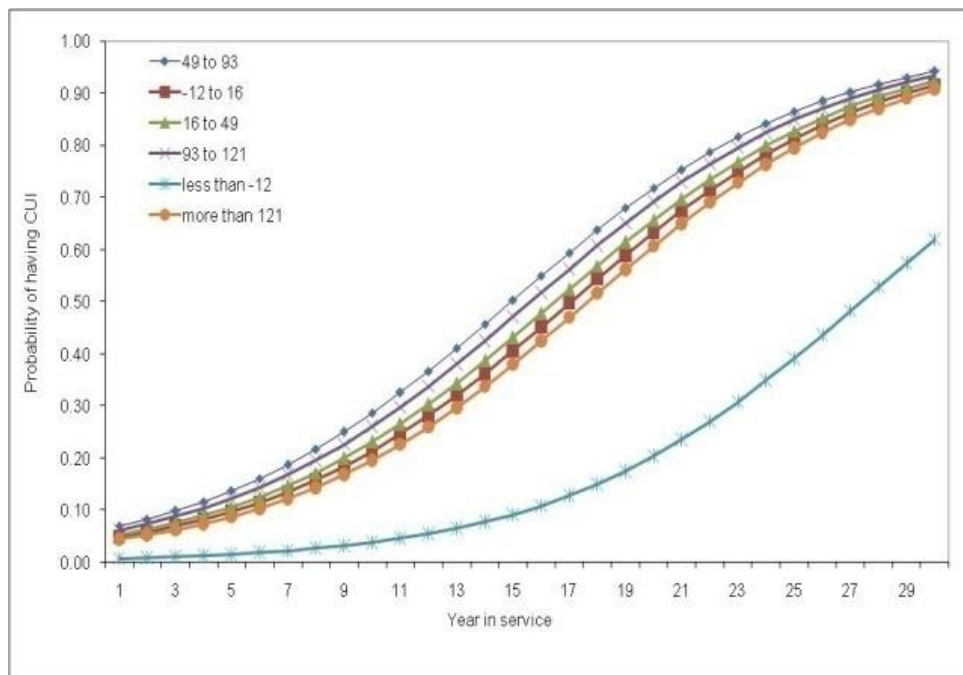
In the analysis, it shows that pipe age and operating temperature are significant factors to determine the probability of CUI occurrence for both small bore and big bore. Insulation type turned to be an insignificant factor for small bore but not for big bore due to the p -value for small bore is higher than $\alpha = 0.05$.

5.1.4 Effect of Pipe Age

The logistic regression coefficient β_1 for pipe age is 0.236 with $\exp(\beta_1) = 1.267$ for small bore and 0.185 with $\exp(\beta_1) = 1.203$ for big bore. This implies that, when pipe age increases by 1 year, the likelihood of small bore pipe will have CUI increases by 26.68% and for big bore is 20.32%. In overall, the trend still follows the API guidelines where operating temperature group 1 (49°C to 93°C) showed the highest probability of having CUI when compared to other temperature groups as shown in Figure 5.1.



(a) Small bore

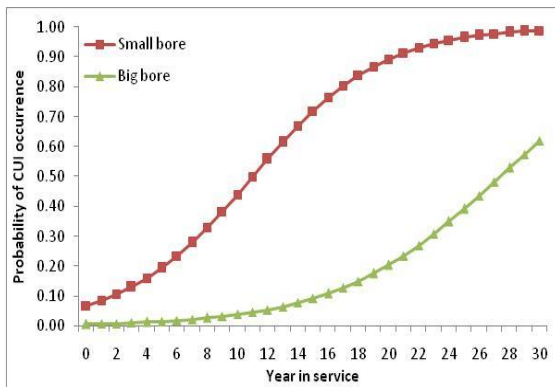


(b) Big bore

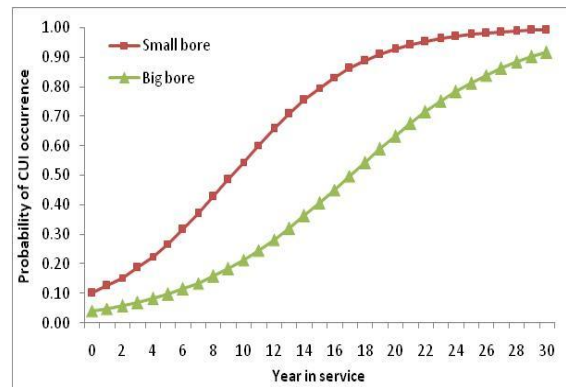
Figure 5.1: Probability of CUI occurrence for each temperature groups for, (a) small bore piping systems and (b) big bore piping systems

5.1.5 Effect of Operating Temperature

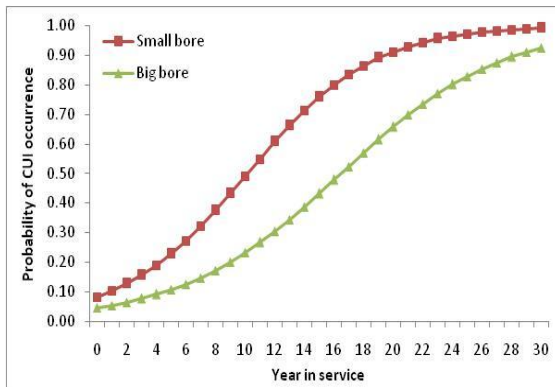
The effect of ranges of operating temperature is as shown in Figure 5.2 and Figure 5.3. The probability for CUI occurrence for six groups of operating temperature for both small and big bore pipes were plotted against years in service. The trend produced replicated the API guidelines where operating temperature group 1 (49°C to 93°C) showed the highest probability of having CUI when compared to other temperature groups. When compared between temperature group 5 (less than -12°C) and temperature group 6 (more than -12°C), group 5 gave higher probability of failure for small bore pipes whereas the results are vice versa for big bore pipes (the failure probability was higher for group 6).



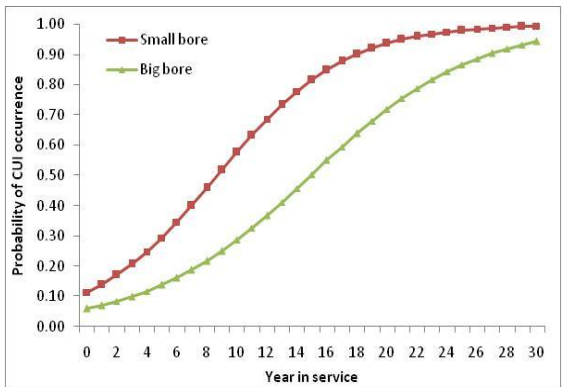
(a) Group 5: Less than -12°C



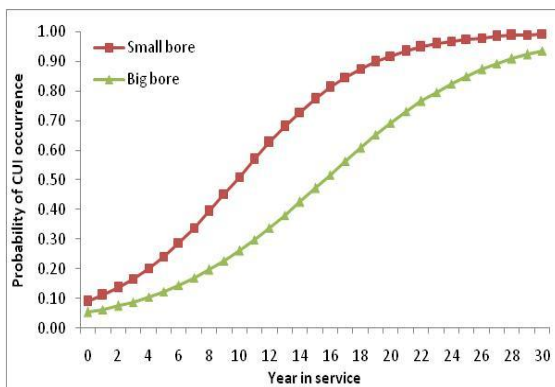
(b) Group 2: -12°C to 16°C



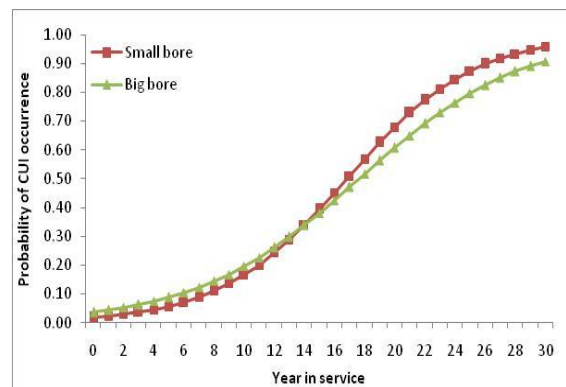
(c) Group 3: 16°C to 49°C



(d) Group 1: 49°C to 93°C

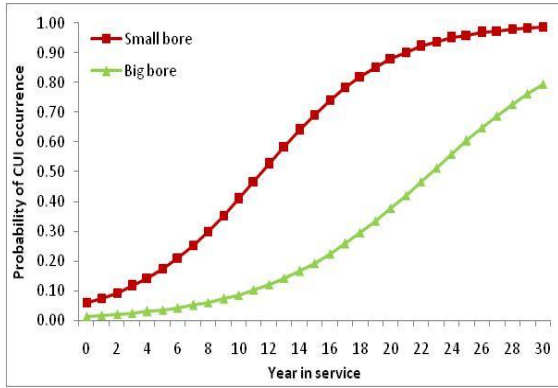


(e) Group 4: 93°C to 121°C

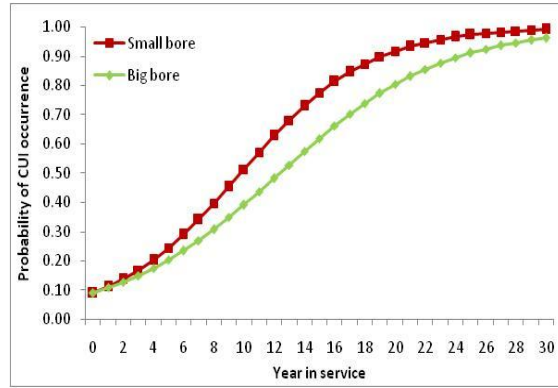


(f) Group 6: More than 121°C

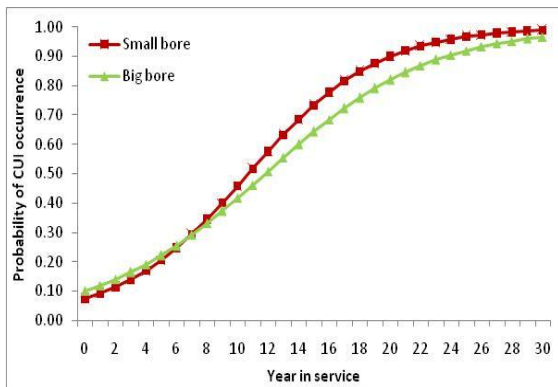
Figure 5.2: Comparison between small bore and big bore piping system for each temperature group (Insulation type = calcium silicate)
(Note: These graphs are plotted based on Table 5.3 and Table 5.7)



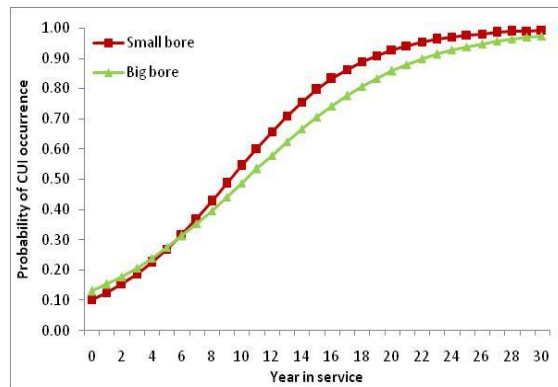
(a) Group 5: Less than -12°C



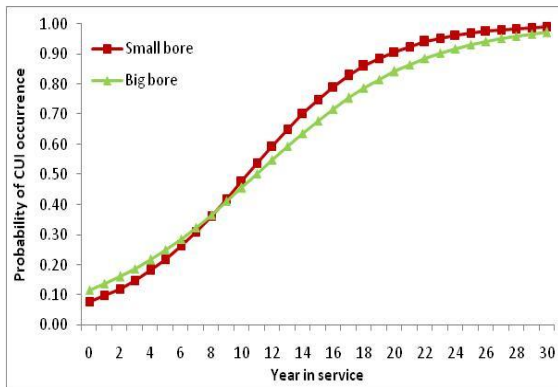
(b) Group 2: -12°C to 16°C



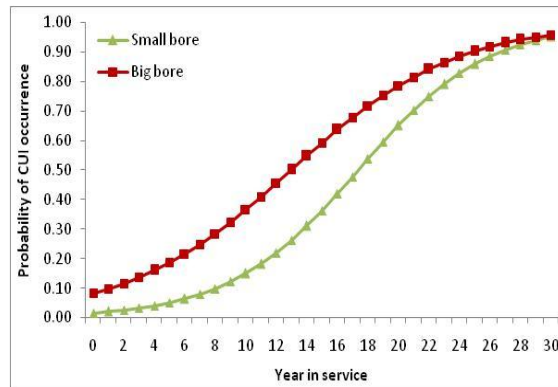
(c) Group 3: 16°C to 49°C



(d) Group 1: 49°C to 93°C



(e) Group 4: 93°C to 121°C



(f) Group 6: More than 121°C

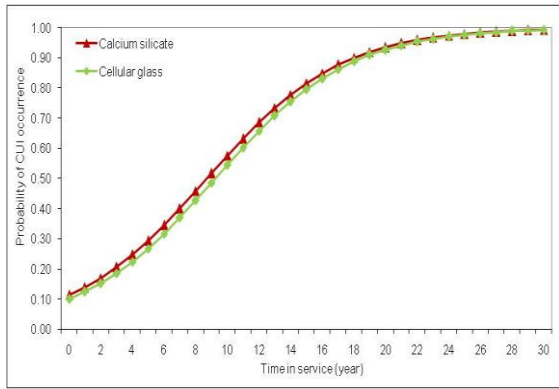
Figure 5.3: Comparison between small bore and big bore piping system for each temperature group (insulation type = cellular glass)

(Note: These graphs are plotted based on Table 5.3 and Table 5.7)

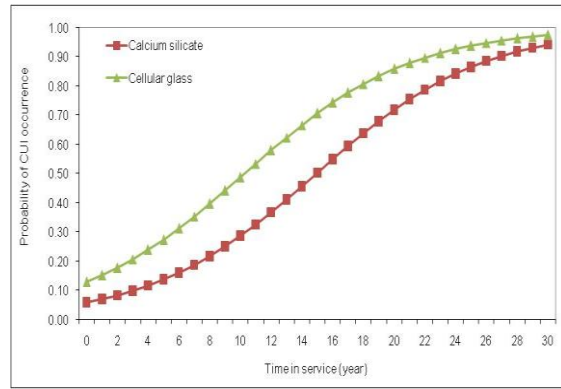
5.1.6 Effect of Insulation Type

Insulation type was found to be an insignificant factor for small bore pipes whereas for big bore pipes, it was a significant factor as shown in Figure 5.4. The result may be due to the following possibility. Insulation for big bore pipes are much easier to get damage due to inspectors or workers may step onto the big pipes in order to enter certain areas which are difficult to access during the daily routine jobs in the plants. By continuously stepping onto the pipe, it will affect the condition of the insulation/cladding itself. Hence, when the insulation is damaged or the sealant is loosed, water easily ingresses into the pipes causing CUI to take place.

Given that the effect of using cellular glass as the insulation material to the odds of pipe deficiency is 1, the effect of calcium silicate on CUI for big bore is $\exp(-0.8644) = 0.4213$. Therefore, pipes with cellular glass shows higher tendency for having CUI instead of calcium silicate. This may be due to the properties of cellular glass itself as it is impermeable to liquid and does not absorb moisture (Silowash, 2010). Calcium silicate acts in different way as it has high physical water absorption function and good porosity. With these characteristics, both serves as advantages for insulation purposes as it can avoid water from being accumulated inside the insulation. Nonetheless, these advantages can counter-back its advantages when the condition of insulation is bad, damaged or broken. In that case, if the insulation material used is made from cellular glass, the water will accumulate onto the pipe surface as this material is not good in absorbing water, and thus it will leave the surface continuously wet. On the other hand, if the type of insulation used is calcium silicate that has high physical water absorption and avoiding heat losses for high temperature, it will reduce the amount of water by absorbing certain amount of it. As a result, the pipe surface will not be as wet as under cellular glass.



(a) Small bore pipes



(b) Big bore pipes

Figure 5.4: Comparison between insulation types for temperature group 1 (49°C to 93°C)

5.1.7 Discussions

Based on the results, the hypothesis of this research is proved as true where small bore and big bore pipes showed different end results where small bore pipes will give higher tendency to experience CUI compare to big bore pipes. Using the field data, it is proved that operating temperature is considered as one of the factors which can contribute directly to the CUI deterioration. This can be explained as follows.

Consider these two pipes operating within the same temperature between -12°C to 16°C as shown in Table 5.11. According to API 581, the default corrosion rate is 0.13 mm/year regardless the pipes size. It showed the small bore pipe will fail first compared to big bore pipe. The reason is due to the diameter of the pipe where small bore pipes will have thinner wall when compare to big bore pipes. With the same rate of corrosion experienced by both small bore and big bore pipes, the time to reach the minimum wall thickness for small bore pipe is faster. Thus, it will cause small bore pipes to be more prone to fail when compared to big bore pipes. This finding also is in agreement with You & Wu (2002) who performed statistical analysis of pressure vessel and piping failures. He found that if the diameter of the pipe is smaller, the probability to have a failure will be higher.

Table 5.11: Example to illustrate why small bore pipe may fail first

	Small bore	Big bore
Line No.	LD-1½"-7004-C1109-C(N31A)	PR-6"-7017-D1101-C(N31A)
Operating temperature	-11°C	15°C
API corrosion rate (mm/year)	0.13	0.13
Pipe wall thickness (mm)	5.08	7.11
Minimum wall thickness (mm)	1.41	2.34
Time to reach the minimum wall thickness (years)	28.23	36.69

This study also produced a mathematical model that provides the likelihood of having CUI for an insulated piping system given the pipe age, operating temperature and insulation type. These CUI factors have been discussed extensively in the literature but no mathematical model has been developed to show the relationship between the likelihood of having CUI and its factors. The results revealed that age and operating temperature have a significant effect on the deterioration of the small bore piping systems whereas for big bore pipes, age, operating temperature and insulation type are important factors.

Intuitively, one knows that the likelihood of having CUI will increase as pipe aging. However, in API 581, the time factor is not being discussed explicitly. The logistic regression has managed to include time as one of the significant model parameters where the probability value can be obtained on certain year in service. Like operating temperature and insulation type, both are the factors for CUI discussed in API 581; nonetheless, the discussion is more towards a guideline. The logistic regression produced a mathematical model to that quantifies the likelihood of having CUI given both factors (i.e. operating temperature and insulation type).

Using a logistic approach also provides a flexible and meaningful model for prediction through the use of both qualitative and quantitative variables. This model can be used to identify the right candidate of pipes for possible inspection, thus eliminating the randomness often associated with inspection/maintenance activity. Subjectivity is reduced as a probability, based on historical inspection records, and the probability values are provided rather than just the possible factors of having CUI, as

stated in API 581. Thus, it results a more systematic way of prediction and offers advantage for inspection monitoring system since inspection engineer can forecast CUI deterioration at any period of time providing more confidence in managing the CUI inspection program.

Naturally, one should be cautioned as the model results will only be as good as the quality of data collected (i.e. the internal visual inspection data). It is recommended that this model needs to be improved by having more parameters, such as the humidity condition, location of equipment/piping etc., as in this analysis, the final model only considered the age, operating temperature group and insulation type as the parameters.

However, the results from the logistic regression model tell us the probability of the pipe may have CUI (i.e. what will be the tendency of having corrosion when we open the insulation), not the probability of failure due to CUI. In other words, the logistic regression model does not tell how severe the corrosion is based on the wall thickness. For that reason, the results generated cannot be compared to Table N-16 in Appendix A in order to categorize the likelihood category for RBI analysis. In conclusion for this section, the logistic regression model can be used as a quantitative model in generating the probability value of having CUI in pipes but the model cannot be applied in quantitative risk assessment. To overcome this matter, another model that has been tested in this study is the degradation analysis model.

5.2 Degradation Analysis

As mentioned earlier in Chapter 3, degradation analysis requires the wall thickness data collected at each TMLs during each inspection period to extrapolate the time-to-failure. In this study, the failure is defined as the time when the wall thickness reaches the minimum wall thickness specified. Extrapolation of the time-to-failure was done by assuming the degradation follows a linear model, Eq. (3.16):

$$d(t) = at + b$$

where $d(t)$ = the wall thickness at time t , t = time and a = the corrosion rate and b = the pipe nominal thickness. Corrosion rate was estimated conventionally using long-term corrosion rate formula, Eq. (4.1):

$$\text{Corrosion rate} = \frac{t_{\text{nominal}} - t_{\text{actual}}}{T}$$

where t_{nominal} = the pipe nominal thickness, t_{actual} = the actual pipe thickness measured at time T and T = number of years in service. Once the time-to-failure were estimated for each TMLs, the data were fitted to an appropriate distribution using Weibull++ software in order to find the distribution parameters.

5.2.1 Case Study

A small-bore, insulated pipe from a local gas processing plant was used to demonstrate the applicability and usefulness of the above technique in assessing the reliability of the piping systems. The insulated small-bore pipe carries high pressure condensate steam where the pipe starts from a heat exchanger (T2-351) to a drum (M2-751) as shown in Figure 5.5. Details on the pipe design and operating parameters are shown in Table 5.12. The corrosion defects and their characteristics became known through a periodic inspection (after opening the insulation).

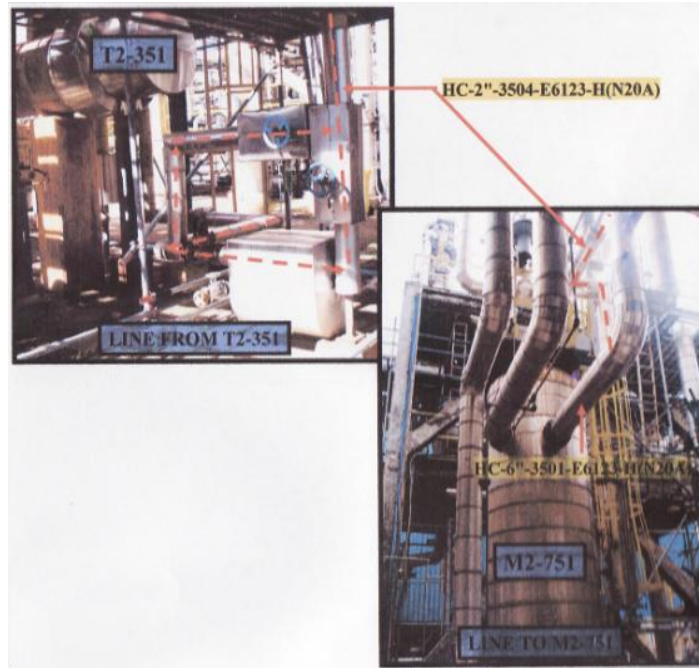


Figure 5.5: Case study of insulated pipe

Table 5.12: Data on pipe

Line No.	HC-2''-3504-E6123-H(N20A)
Line Route:	From T2-351 to HC-6''-3504-E6123-H(N20A)
Design Pressure:	4500 KPA
Operating Pressure:	3900 KPA
Design Temperature:	395°C
Operating Temperature:	249°C
Line type	Steam condensate line

32 data points taken from 32 different TMLs along the pipe were used for this degradation analysis. Corrosion rates at each TMLs were calculated as well as the time-to-failure as shown in Table 5.13. Then, the time-to-failure data generated were analyzed using Weibull++ software in order to find the distribution parameters. Table 5.14 shows that the data fitted well in the lognormal distribution, followed by the exponential 2-parameter and Weibull distributions (in that order) based on the likelihood values.

Table 5.13: Time-to failure data at each TML

Location	Calculated corrosion rate (mm/yr)	Time-to-failure (year)	Location	Calculated corrosion rate (mm/yr)	Time-to-failure (year)
1	0.111	71.4	17	0.142	20.6
2	0.142	20.6	18	0.144	20.1
3	0.169	14.9	19	0.120	27.2
4	0.183	12.7	20	0.274	3.4
5	0.115	28.9	21	0.103	34.3
6	0.142	20.6	22	0.155	17.7
7	0.169	14.9	23	0.053	79.9
8	0.142	20.6	24	0.132	23.3
9	0.142	20.6	25	0.072	55.3
10	0.142	20.6	26	0.077	51.0
11	0.169	14.9	27	0.053	79.9
12	0.169	14.9	28	0.053	123.0
13	0.142	20.6	29	0.051	84.9
14	0.142	20.6	30	0.077	51.0
15	0.142	20.6	31	0.051	84.9
16	0.169	14.9	32	0.077	51.0

Table 5.14: Results for each statistical distribution

Distribution	Parameter	Likelihood values
Lognormal	$\mu = 3.3206, \sigma = 0.7414$	-142.071
Exponential 2-parameter	$\lambda = 0.0310, \gamma = 3.400$	-143.742
Weibull	$\beta = 1.729, \eta = 38.157$	-146.304

The time-to-failure data fitted best in the lognormal distribution, where the median life, $T_{50} = e^{\mu} = e^{3.3026} = 27.7$ years (i.e. the median time to failure is 27.7 years). (Note that the median life is the value of the random variable that has exactly one-half of the area under the probability density function to its left and one-half to its right.). The results matched with the discussion in the literature which highlighted that one of the degradation processes that follow the lognormal distribution is corrosion and, in general, failures resulting from chemical reactions or processes empirically follow this distribution.

If one were to use the 2 parameter exponential distribution, it can be interpreted as no failure will occur in 3.40 years after the first installation and the beyond 3.40 years,

the failure rate is estimated to be 0.031 failure per year (based on the assumption of constant failure rate). If Weibull distribution were to be used, it revealed that the failure rate of the pipe is increasing (with $\beta = 1.729$) and the life at which 63.2% of units will fail will be at 38.2 years. Figure 5.6 shows the three distributions fitted well to the time-to-failure data and Figure 5.7 shows the graphs of the probability of failure vs. years in service for all the three distributions.

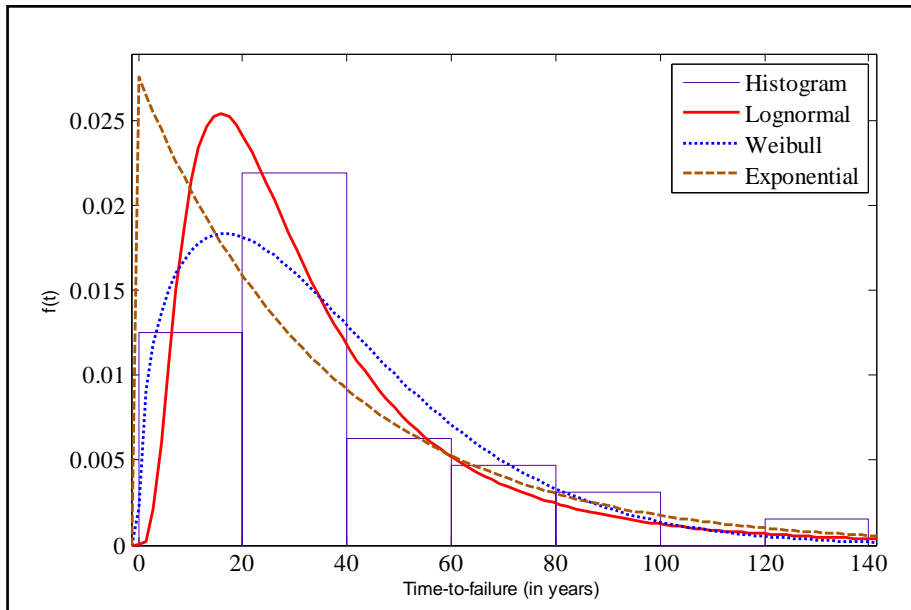


Figure 5.6: Distribution fitting for the time-to-failure data

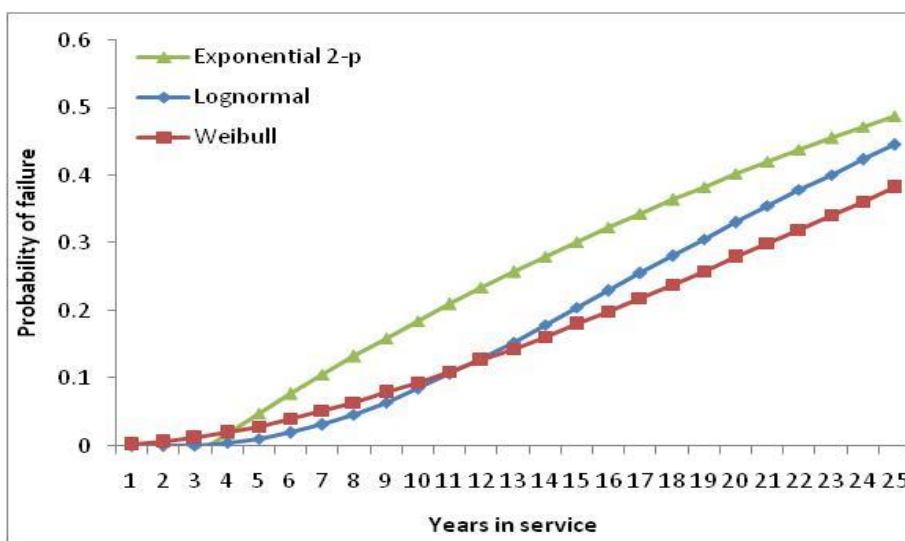


Figure 5.7: Probability of failure generated by assuming a linear degradation model

5.2.2 Results

A sample of 30 pipes were collected at various temperatures and the results of the analysis showed that either the lognormal distribution or the Weibull distribution gave a very good fit to the time-to-failure data extrapolated from a linear degradation model (i.e. adopted from API 581). This is because the likelihood values generated by these two distributions were greater when compared to other distributions). Table 5.15 shows the details of the results.

Table 5.15: Sample results at various temperatures

Operating temperature (°C)	Weibull distribution			Lognormal distribution		
	β	η	Likelihood value	μ	σ	Likelihood value
-39	0.920	238.12	-158.70	4.877	1.415	-145.87
15	1.192	214.47	-94.75	4.917	1.015	-94.74
36	1.326	285.51	-326.86	5.231	0.941	-329.34
93	2.184	70.36	-122.63	4.004	0.582	-120.86
290	0.926	431.64	-133.86	5.481	1.384	-129.21

5.2.3 Discussions

Reliability analysis based on time-to-failure data are often hampered by the lack of observed failures. The probabilistic model has demonstrated an alternative approach to the time-to-failure data in order to assess the piping system reliability subject to CUI. Rather than just developing a degradation model of corrosion as normally being practiced in the plants, the model also seeks the resulting lifetime model. The lifetime distribution model can be used to predict the probability of failure of the insulated piping system at any point in time without having to estimate the corrosion rate. Several interesting points can be highlighted using this analysis:

- The time-to-failure data for CUI which is based on a linear degradation model obeys either the lognormal distribution or Weibull.

- Based on the Weibull distribution in Table 5.15, the shape parameter β for very cold or very hot piping systems (operating temperature $< -12^{\circ}\text{C}$ or $> 121^{\circ}\text{C}$, respectively) is less than 1 which indicates that the failure rate decreases over time. Up to a point, the failure rate will become constant. Planned replacement has no advantage in these cases because the failure will occur at random.
- For piping systems that operate between -12°C and 121°C , the shape parameter β is more than 1 which implies that the failure rate increases over time. The increasing failure rate indicates wear out such as corrosion and such pipes will have higher risk of failure and thus frequent inspection interval is recommended.

In overall, the proposed analysis framework intends to simplify the modeling process so that the available data can be fully utilized for prediction purposes. This study has also linked a practitioner's selected degradation model and the resulting lifetime model with the objective to predict quantitatively the failure probability. The model can be applied easily provided the number of wall thickness data collected is sufficient so that the analysis made is sound and credible. However, to have abundance of wall thickness data for insulated pipes is not always being the case, which means the degradation analysis cannot be carried out. Therefore, the big question is how to assess the probability of failure quantitatively? Another model that can be employed by taking the advantage of using the wall thickness data as well as the design and operating data is the structural reliability analysis.

5.3 Structural Reliability Analysis

5.3.1 Model verification

The FORM algorithm developed using Microsoft Excel was verified using two case studies published in the literature (Cardoso et al., 2008; Teixeira et al., 2008). Both case studies were not about CUI; however, they were on assessing reliability of pipelines with corrosion defect. The developed FORM model produced the same

results as published in the papers. For details of the validation results, refer to Appendix D.

5.3.2 Establish the distribution

For structural reliability analysis, the probability distribution for each basic random variable has to be determined. For operating pressure, operating pressure data were analyzed using JMP software, statistical software to establish the probability distribution. Figure 5.8 shows the examples of the operating pressure distributions for 2 insulated pipes. The analysis shows that the operating pressure follows normal distribution with COV of 0.02.

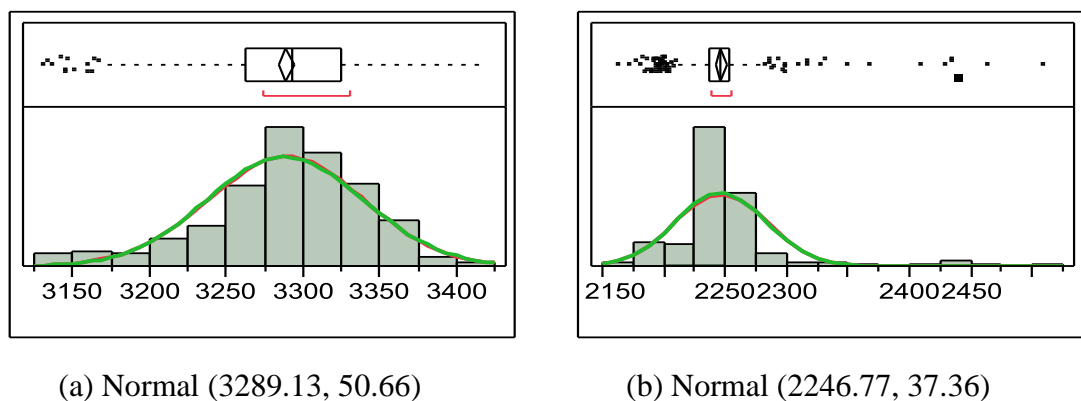
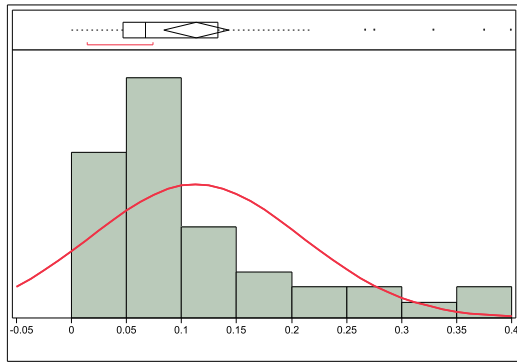


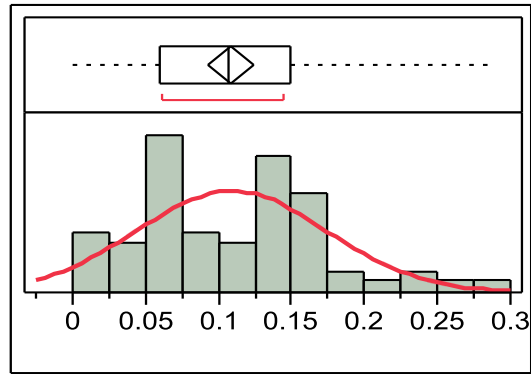
Figure 5.8: Probability distribution for operating pressure taken at two different locations; (a) 3PI5003.PV and (b) 3PI4502.PV

Estimation for probability distribution and its parameter for CUI corrosion rate are done using two methods, by (1) fitting the distribution and (2) the bootstrap resampling method, based on the number of data available. The temperature group 3 and 6 data were fitted to an appropriate distribution since the number of data is reasonable (more than 30 data points) to conduct the distribution fitting method as shown in Figure 5.9. For other groups, the bootstrap resampling method has to be employed since data is inadequate. Figure 5.10 shows the empirical probability distributions produced by this method.



Normal(0.11314,0.096)

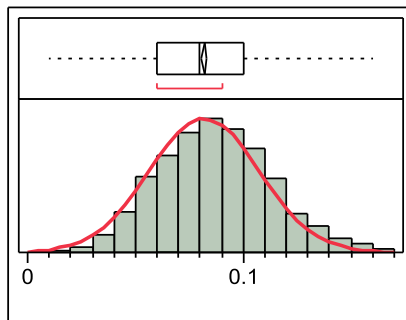
(a) Distributions for Group 3 (16°C to 49°C)



Normal(0.10893,0.065)

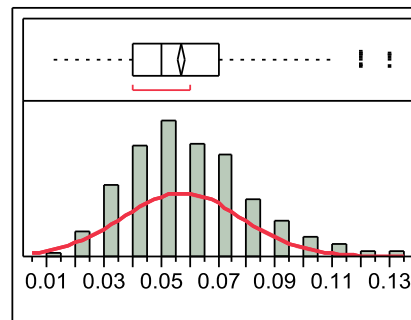
(b) Distributions for Group 6 (more than 121°C)

Figure 5.9: Probability distribution of CUI corrosion rate established using the distribution fitting method for 2 different operating temperatures



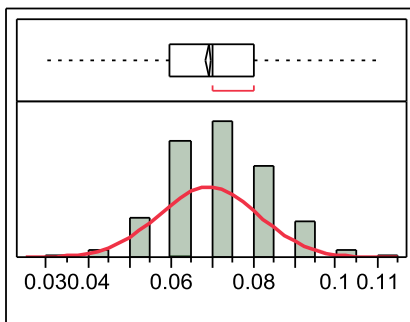
Normal (0.081,0.075)

(a) Distributions for Group 1 (less than -12°C)



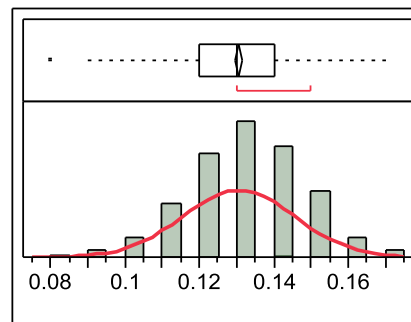
Normal (0.057,0.062)

(b) Distributions for Group 2 (-12°C to 16°C)



Normal (0.070,0.036)

(c) Distributions for Group 4 (49°C to 93°C)



Normal (0.130, 0.047)

(d) Distributions for Group 5 (93°C to 121°C)

Figure 5.10: Probability distribution of CUI corrosion rate established using the bootstrap method

Once the statistics are known then it will be used for the data analysis of FORM model. Table 5.16 summarizes all the results for corrosion rate.

Table 5.16: API 581 corrosion rate vs. estimated corrosion rate

Temperature range (°C)	API Corrosion Rate* (mm/yr)	90% Confidence Interval			Std Dev of Corrosion Rate	Coefficient of Variation (COV)
		Mean of Corrosion Rate (mm/yr)	Lower Bound	Upper Bound		
Less than -12	0	0.081	0.040	0.123	0.075	0.949
-12 to 16	0.127	0.057	0.027	0.095	0.062	1.094
16 to 49	0.0508	0.113	0.083	0.142	0.096	0.850
49 to 93	0.254	0.070	0.051	0.089	0.036	0.512
93 to 121	0.0508	0.130	0.106	0.152	0.047	0.364
More than 121	0	0.109	0.093	0.125	0.065	0.596

* The corrosion rate is the corrosion rate in marine environment (API, 2003)

To check whether the estimated corrosion rate is difference when compare to API corrosion rate, Student-t test was used. Student-t test is a statistical hypothesis test in which the test statistic is assumed to follow a Student's t distribution if the null hypothesis is true. In this case, the following hypothesis is made:

H_0 : The means of the corrosion rate for both groups are equal.

H_A : The means of the corrosion rate for both groups are not equal.

Using the paired t -test, the two-tailed p -value equals 0.8112. By conventional criteria, the difference is considered to be not statistically significant which means do not reject the null hypothesis. In other words, the means of the corrosion rate for both groups are equal. It can be implied that the corrosion rate estimated using the field data can be used in the structural reliability analysis especially for pipes with temperature operating below -12°C or higher than 121°C where API corrosion rate are supposed to be zero. When corrosion rate is zero, the structural reliability analysis cannot be conducted.

The results generated using field data look promising as a mean to quantitatively predicting the probability of failure. The bootstrap resampling method used also provides a way to generate the empirical distribution for the corrosion rates. As what has been mentioned by Chernick (2008, pg 173), "Although we have good reasons not to trust the bootstrap in very small samples and theoretical justification is asymptotic,

the result were surprisingly good even for sample sizes as small as 14 ...A main concern in small samples is that with only a few values to select from, the bootstrap sample will under-represent the true variability since observations are frequently repeated and bootstrap samples, themselves, can repeat.”.

5.3.3 The influence of the limit state function

The probability of failure generated was based on the limit state function proposed by Khan et al. (2004). The next question is whether the results change if a different limit state function is used. As mentioned earlier, another limit state function that is typically used is the failure function that is defined as the difference between the pipe failure pressure P_f and the pipe operating pressure P_{op} . Note that all the variables in the modified B31G failure pressure model are the same as the data in the thinning model except that the modified B31G failure pressure model requires the axial length of the corrosion defects, l . In this analysis, l is assumed to be constant.

Figure 5.11 shows the results of the application of the FORM algorithm to compute the pipe failure probability using both the thinning model and the modified B31G (i.e. Eq. (4.4) and Eq. (4.5)). A time interval of 25 years was considered. A normal distribution was assumed for the load and resistance variables for both models. The analysis has been carried out with $l = 100$ mm, $l = 200$ mm and $l = 300$ mm.

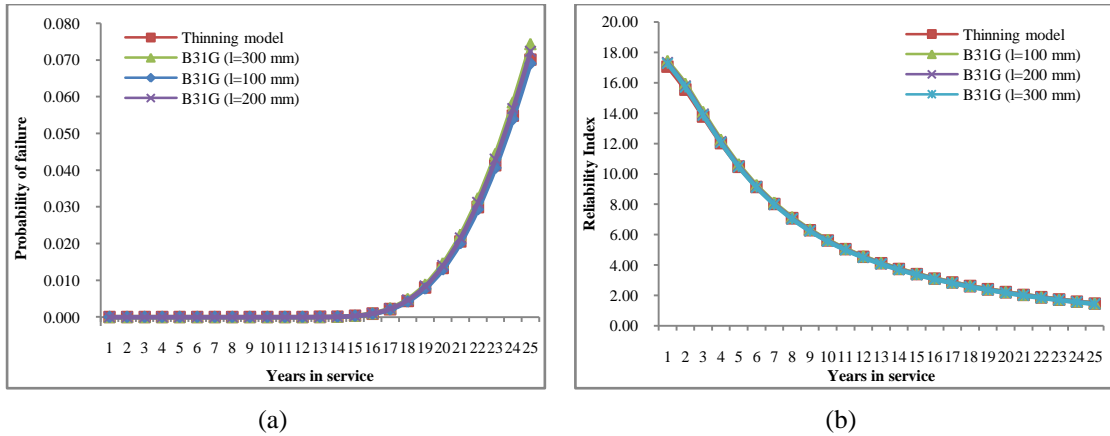


Figure 5.11: (a) Evolution of pipe failure probability with time for thinning model and the modified B31G failure pressure model. (b) Evolution of pipe reliability index with time for thinning model and the modified B31G failure pressure model.

The results in Figure 5.11 show that both models used to predict the failure probabilities give similar pipe failure probabilities. Even with different axial length of defect, the similar pipe failure probabilities are produced. The advantage to use the thinning model over the modified B31G is that the equation does not require the axial length of corrosion defect where in most cases (in practical), the corrosion defect length is seldom measured.

5.3.4 The influence of the reliability algorithm

The results shown in Figure 5.12 were obtained using the FORM algorithm to compute p_f . As Figure 5.11 shows, the Monte Carlo simulation technique gives results that closely approach that obtained by FORM (the thinning model has been used in this analysis). Although the Monte Carlo technique produce similar results for both models and variable distribution types considered in this study, important implementation and performance details have to be considered to select the most suitable algorithm when a probability-based analysis is done. The advantage of using Monte Carlo simulation is it is easily implemented and does not require partial differentiation of the limit state function; therefore, any limit state function can be used with this algorithm. The major drawback of this method is the lack of computing

efficiency resulting from the large number of trials (about 10^5) required in order to ensure an accuracy approaching that obtained using the FORM. In this case 10,000 trials were found to be enough in order to for converge to take place.

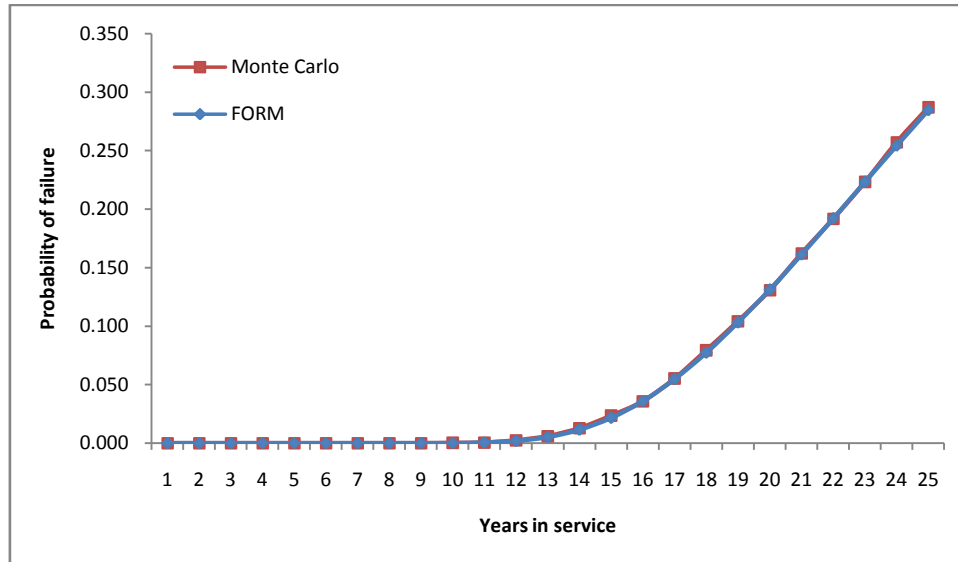


Figure 5.12: FORM vs. Monte Carlo algorithms for generating the failure probability

5.3.5 The influence of COV of the load and resistance variables

It is obvious that the pipe reliability is affected by the degree of uncertainty present in the random variables. COV of a random variable is a measure of uncertainty present in the random variable. Therefore, it is necessary to undertake a sensitivity study on parameters in order to demonstrate the effect of variation in COV of random variable on the pipe reliability. COV is the ratio of standard deviation to mean of a random variable, the variation of COV will result in the behavior of parameter. The sensitivity of the pipe reliability to the COV of the load and resistance variables was assessed using COV value ranges between 0 and 1. The reliability indices were evaluated for various service lives for the above-mentioned pipe in the case study. Figure 5.13 shows the influence of COV on the load and resistance parameters on the results of the probabilistic analysis.

In this analysis, the thinning model was used and the load and resistance variables were assumed to be normally distributed. The pipe reliability was found to be:

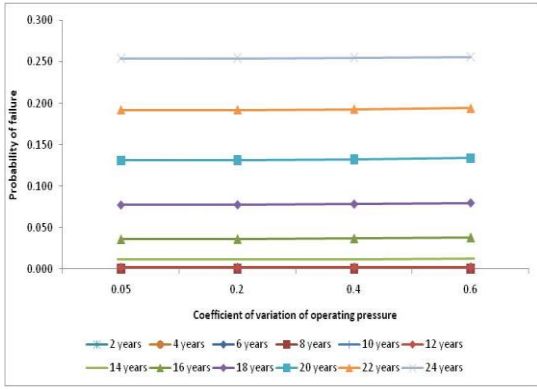
- Very sensitive to the pipe wall thickness and corrosion rate.
- Moderately sensitive to pipe material strength.
- Almost insensitive to operating pressure, pipe diameter.

From the analysis, it is found that the pipe reliability is almost insensitive to COV of operating pressure and the pipe diameter at any service life. It was also found out that material strength appears to make a significant relative contribution to the pipe failure initially; however, its relative contribution diminishes gradually with time.

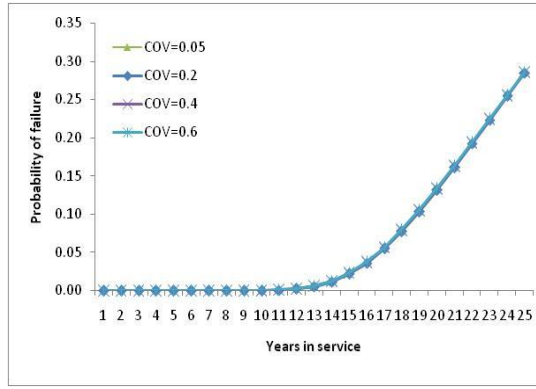
It is observed from the results that the pipe failure probability increases with increased values of COV of pipe wall thickness and corrosion rate. This means that, even if the mean values of the random variables remain unchanged, the probability of failure of the pipe increases with increased values of COV of the pipe wall thickness and corrosion rate.

From Figure 5.13 (i) and (j), it is seen that the change in the failure probability with respect to the change in COV of corrosion rate for low service life is not significant. However, the sensitivity increases gradually with increased years in service. This implies that an accurate or near accurate estimate of the COV value of defect depth is needed for when service periods is longer, otherwise the evaluated failure probabilities would not be so realistic. Moreover with increased years in service, the depth of defect (i.e. wall loss) increases, resulting in a decrease in pipe wall thickness and hence the capability of pipe to resist the effect of stresses generated by external loads is reduced. In other words, this increases the severity of the circumferential stress leading to an increase in failure probability of the pipe.

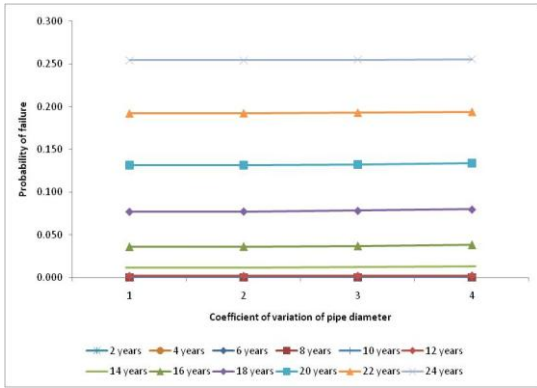
From Figure 5.13 (e) and (f), it can be seen that the failure probability is very sensitive for the values of COV of the pipe wall thickness. The sensitivity increases gradually with increased years in service but it never loses its significance even at the high exposure periods.



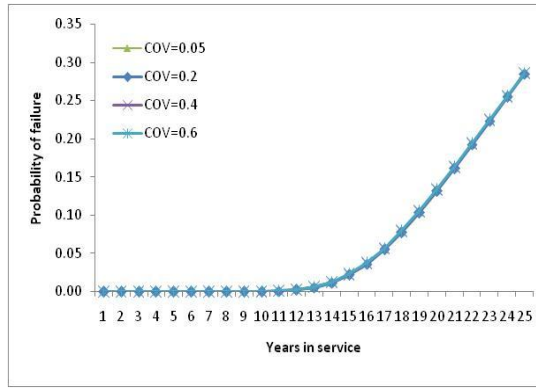
(a)



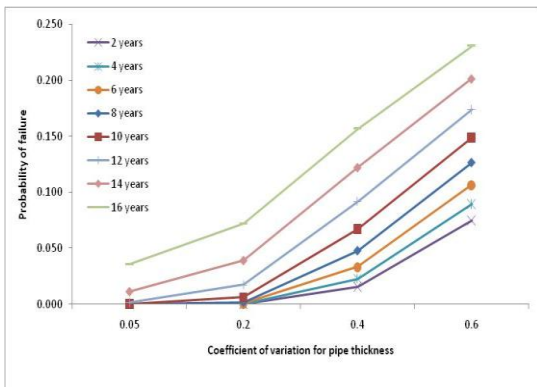
(b)



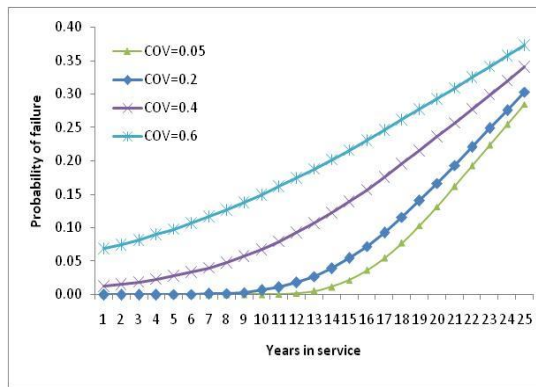
(c)



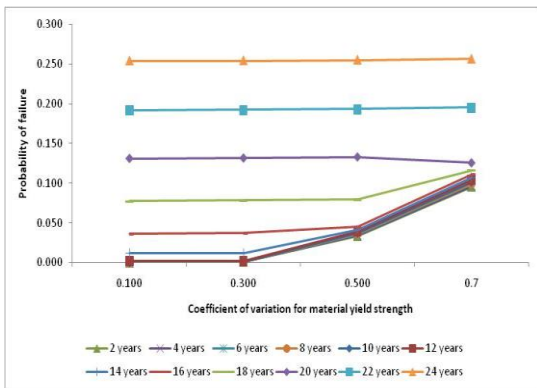
(d)



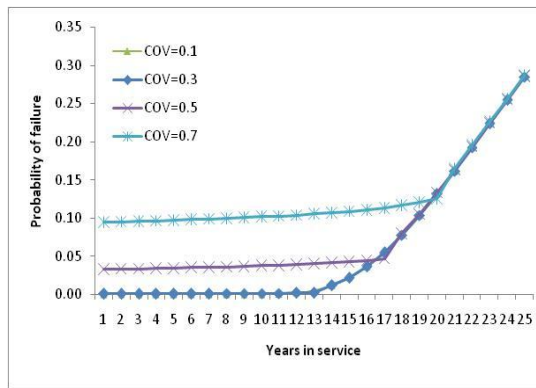
(e)



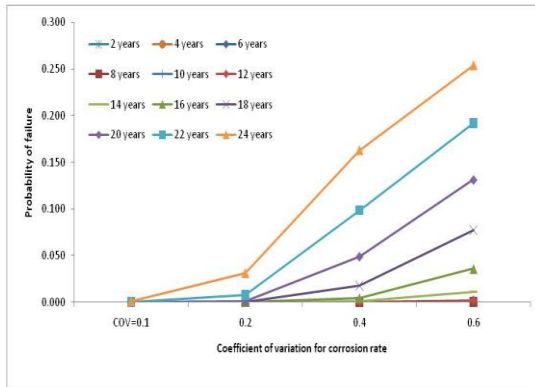
(f)



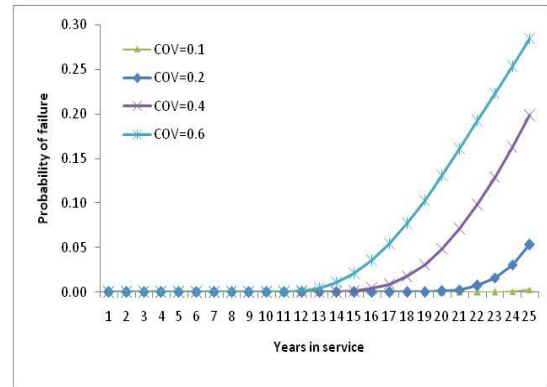
(g)



(h)



(i)

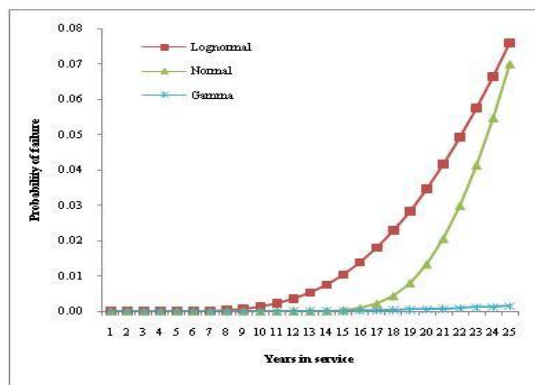


(j)

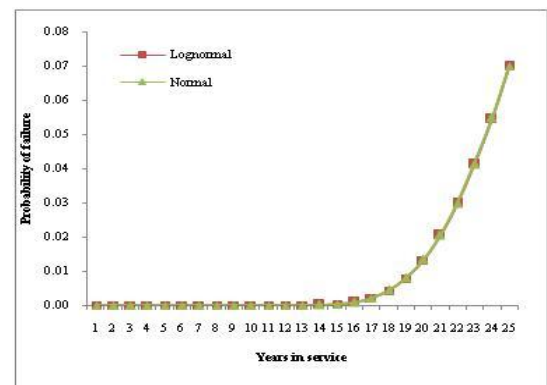
Figure 5.13: Sensitivity analysis for: (a) – (b) COV of operating pressure, (c) – (d) COV of pipe diameter, (e) – (f) COV of pipe thickness, (g) – (h) COV of material strength, and (i) – (j) COV of corrosion rate.

5.3.6 The influence of the probability distribution of the load and resistance variables

The influence of the distribution type on thickness and corrosion rate on the pipe failure probability is shown in Figure 5.14. Figure 5.14 (a) shows the distribution type of corrosion rate is of first importance on the pipe safety in the future. The lognormal distribution produces the highest failure probabilities, which is as expected since the tails of the distributions have on the computed failure probability. Figure 5.14 (b) shows that there is no big influence on the probability of failure by having difference types of distributions for pipe wall thickness.



(a) Distribution of corrosion rate



(b) Distribution of pipe wall thickness

Figure 5.14: The effect of different probability distribution on the failure probability

5.3.7 Case study

Another small-bore, insulated pipe was used to demonstrate how the structural reliability analysis the applicability of the above technique in assessing the reliability of the piping systems. It is a cold pipe where the medium is propane refrigerant, operating at -39°C , however, intermittently used as shown in Figure 5.15. Table 5.17 shows the pipe details. The data employed to run the analysis are shown in Table 5.18.

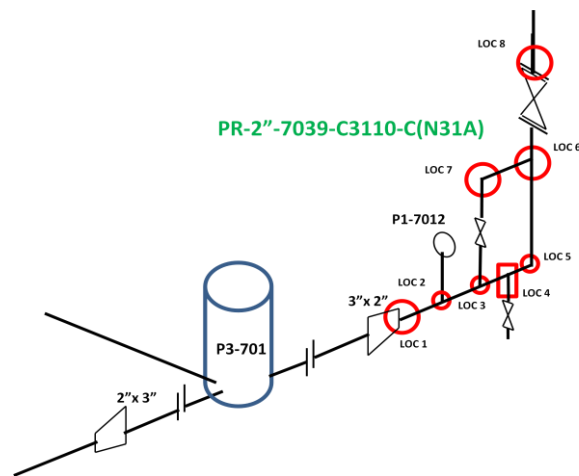


Figure 5.15: Case study of insulated pipe

Table 5.17: Data on pipe

Line No.	PR-2-7039-C3110-C(N31A)
Line Route:	From P3-701 to Spec Brk
Design Pressure:	2100 KPa
Operating Pressure:	750 KPA
Design Temperature:	$-46/60^{\circ}\text{C}$
Operating Temperature:	-39°C
Line type	Propane refrigerant line

Table 5.18: Parameter for limit-state function with mean and variance

Symbol	Parameters	Mean	Variance
S	Yield stress (MPa)	240	11.2896
d	Material thickness (mm)	5.54	0.0767
D	Outside diameter of pipe (mm)	60.3	1.0508
C	Operating pressure (MPa)	0.75	0.0067
P	Corrosion rate (mm/yr)	0.079	0.0039

The plots of the failure probability and the reliability index against year in service (t) are presented, as shown in Figure 5.16 and 5.17, to draw the inferences. It is observed that the failure probability generated for the first 15 years are very small. However, after the first 15 years in service, the probability of failure increases exponentially. It can be seen from Figure 5.16, after 15 years in service, the failure probability of the pipe is 6.24×10^{-6} with the reliability index of 4.37. Comparing the probability value with the failure probability categories in Table N-16 (Appendix A), the pipe is now in the likelihood category 3 which is medium category of failure probability.

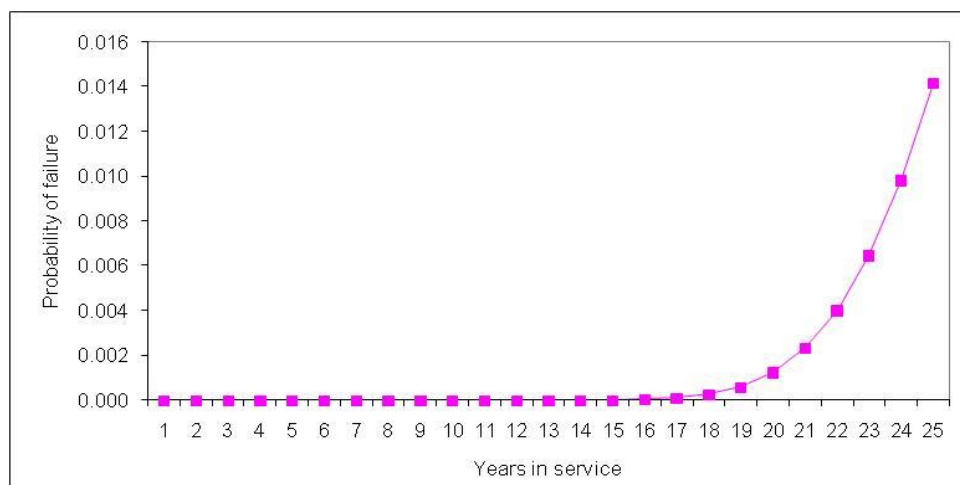


Figure 5.16: Failure probability plot

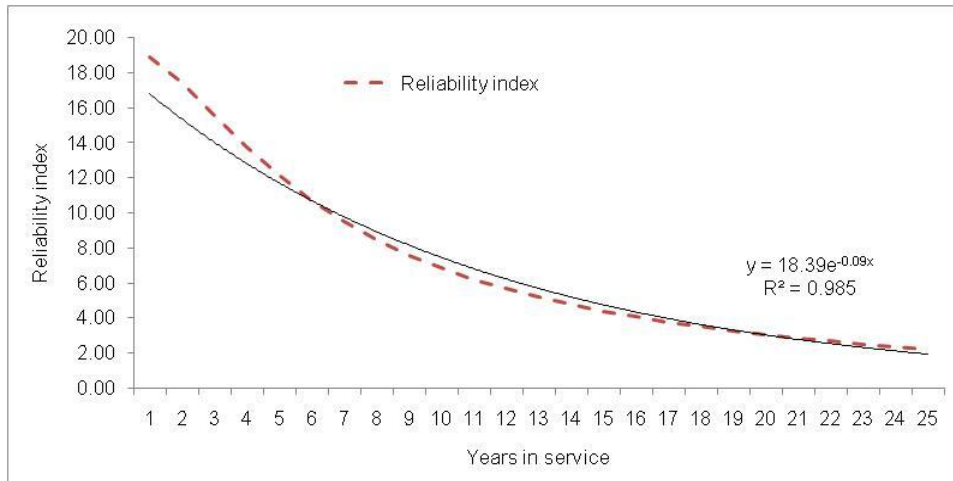


Figure 5.17: Reliability index vs. years in service

It can be seen from the reliability index plotting in Figure 5.17 that as the year in service increases, the reliability index decreases exponentially. This is as expected and may be explained in the following way. With increased year in service, the corrosion defect increases, and hence the pipe capability to resist the effect of stresses generated by the loads is also reduced. In other words, this increases the severity of the circumferential stress leading to an increase in the pipe failure probability.

The graph in Figure 5.17 can be used to plan effective and economic inspection, repair and replacement programs. Not only that, this graph can be used to set effective remaining service life. For example, if the hypothetical minimum acceptable value of reliability index is set at 3, then it can be said that the remaining service life of this pipeline is (20 - 15) years, i.e. 5 years. After the period of the remaining life, even if it appears that the pipeline has not failed, it would not be safe to use it. For safety reasons, it would be wise for the pipe to be abandoned, repaired or replaced, in order to decrease its failure probability if further service is required.

5.3.8 Discussions

A study on the reliability assessment methodology for insulated piping systems subject to CUI has been carried out for the purpose of RBI. This study was needed to

establish RBI program for piping systems subject to CUI in a more quantitative way. Thinning model proposed by Khan et al. (2003) was employed for estimating the failure probability of the insulated pipes containing corrosion defects as well as the remaining strength of those pipes. The results generated by the thinning model were validated with the standard failure pressure model, the modified B31G. FORM was adopted for evaluating the limit state function and was validated using Monte Carlo simulation. The main results of this study lead to the following conclusions:

- Both the thinning model and the modified B31G predicted similar values of the failure probabilities.
- FORM and Monte Carlo simulation reliability algorithms produce similar results when the limit state function can be linearized and the load and resistance variables have normal probabilistic distributions. In this case, with 10,000 runs, it is already reaching the convergence.
- The pipe failure probability increases with increased service life and that the rate of change of pipe failure probability also increases gradually with the increase service life.
- At low service life (about 10 to 12 years in service), the pipe reliability is almost insensitive to the input variables but the sensitivity of the failure probability estimate increases gradually with increased service life.
- At low service life, the pipe reliability is almost insensitive to COV of the load and resistance variables. However, special care must be taken in characterizing accurately COV of the variables if the reliability of pipes is assessed for longer years in service. Moreover, it is pointed out that if the reduction in pipe safety is assessed for long service times, then special care must be taken in charactering COV of the variables (1) corrosion rate, (2) pipe wall thickness (in that order).
- At any service life, the pipe reliability is almost insensitive to pipe diameter, material strength and pipe operating pressure.
- If the probabilistic distribution of a load and resistance is not experimentally available, the sensitivity of the pipe reliability to this variable is the key to assume its distribution type.

- The probabilistic analysis of a pipe must be performed independently for deep and shallow defects in order to ensure a correct repair strategy for shorter and longer years in service.
- It is observed that the pipe falling under very high category indicating the most significant pipe needs to be investigated through RBI.
- The last important point is the interest to better estimate the coefficient of variation associated to corrosion rate because it is a parameter of great influence towards numerical simulations.
- Numerical simulations have been performed and allow describing the evolution of the safety index of the insulated pipes with time.
- The graph, reliability index versus years in service would be a good guide to set the effective remaining service life. After this period, even if it appears that the pipe has not failed, it would not be safe to use it. For reasons of safety, it would be wise for the pipe to be repaired or replaced, in order to decrease its failure probability if further service is required of it. This graph will be used to plan effective and economic inspection, repair and replacement programs.

From the research presented herein, it can be concluded that the application of FORM is very promising in estimating quantitatively the failure probability of insulated piping systems for RBI analysis.

5.4 Continuous-Time Markov Model

5.4.1 Model Validation

A three-discrete-state, continuous-time Markov model was employed in this study, as shown in Figure 5.18. The model describes the condition of the insulated piping systems based on the severity of the corrosion defects which can be categorized into three states as shown in Table 5.19. The pipe is assumed to be in any one of the three states reflecting the progressive stage of CUI. This model assumes that the insulated piping system can either stay in its current state or deteriorate to some lower state. In

the presence of repair/maintenance activities, then the pipes is assumed to go back to a better state.

Table 5.19: Description for the 3-state Markov model

State	Definition
1	d less than t_1
2	d is between t_1 and t_2
3	d is more than t_2

Note: d = the depth of corrosion, $t_1 = t_2 - \frac{t_2}{2}$, $t_2 = t_{nominal} - t_{minimum}$

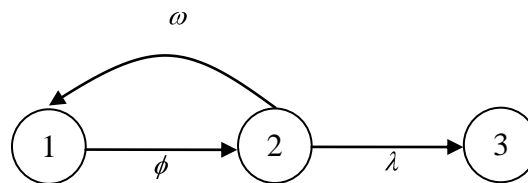


Figure 5.18: Proposed three-state Markov model

The differential equations developed for the three-state Markov model was solved analytically using Laplace transforms (refer to Appendix C for the solutions) and once such solutions were obtained, the calculation was performed via spreadsheet yielding the time dependent probabilities of the piping at each state. To validate the analytical closed form solutions to these differential equations, the probability values generated were compared to the results generated using MATLAB (i.e. solving it numerically). Both values solved using spreadsheet and MATLAB were equal, thus proving that the differential equations solved using Laplace transforms and putting the equations in the spreadsheet was validated.

5.4.2 Estimation of transition rates ϕ , λ and ω

The continuous-time Markov model requires the transition rates from State 1 to State 2, ϕ and from State 2 to State 3, λ , which were determined using the structural reliability analysis based on the limit state functions discussed in Chapter 3. The first limit state function was used to estimate ϕ and can be defined as:

$$\text{LSF1: } g(x) = t_1 - (0.125t_{nominal} + CR \times T) \quad (3.56)$$

where $t_1 = t_2 - \frac{t_2}{2}$ (in mm), $t_2 = t_{nominal} - t_{minimum}$, $t_{nominal}$ = pipe nominal wall thickness, $t_{minimum}$ = minimum wall thickness specified, CR is the corrosion rate (in mm) and T is the time of inspection which usually 10 years.

The second limit state function to estimate the transition rate λ represents transition rate from state 2, which has already crossed the detectable range t_1 , to the state 3, in which the wall thickness is beyond the minimum wall thickness allowed t_2 . The LSF for this case would be

$$\text{LSF2: } g(x) = t_2 - [t_1 + CR \times T] \quad (3.57)$$

Note that, in this model, the State 3 does not specify the actual leak, but represents a stage where the corrosion defect reaches the minimum wall thickness. First-order reliability method (FORM) was employed to estimate the transition rates.

To illustrate how the approximations of transition rates were done, the same example of pipe in Section 5.3.7 was used. Running FORM using both limit state functions yields the results shown in Table 5.20 and Table 5.21. The reliability data for the first limit state function were fitted into the exponential curve $f(t) = e^{-\lambda t}$ using MATLAB and the results showed that the estimated $\lambda = 0.03627$ per year (with 95% confidence bounds between 0.03101 and 0.04153) and $R^2 = 0.8837$ as shown in Figure 5.19 (a). For the second limit state function, the reliability data were also fitted into the exponential curve as shown in Figure 5.19 (b) and the results showed that the estimated $\lambda = 0.02368$ (with 95% confidence bounds between 0.02109 and 0.02627) and $R^2 = 0.8918$.

Table 5.20: Reliability data generated from the first limit state function.

Time	Reliability	Time	Reliability
1	1.000	11	0.837
2	1.000	12	0.788
3	1.000	13	0.741
4	1.000	14	0.695
5	1.000	15	0.653
6	0.997	16	0.614
7	0.986	17	0.579
8	0.963	18	0.548
9	0.929	19	0.519
10	0.885	20	0.507

Table 5.21: Reliability data generated from the second limit state function.

Time	Reliability	Time	Reliability
1	1.000	16	0.883
2	1.000	17	0.852
3	1.000	18	0.821
4	1.000	19	0.790
5	1.000	20	0.760
6	1.000	21	0.730
7	1.000	22	0.701
8	1.000	23	0.674
9	0.999	24	0.648
10	0.995	25	0.624
11	0.988	26	0.600
12	0.976	27	0.579
13	0.959	28	0.558
14	0.937	29	0.539
15	0.911	30	0.521

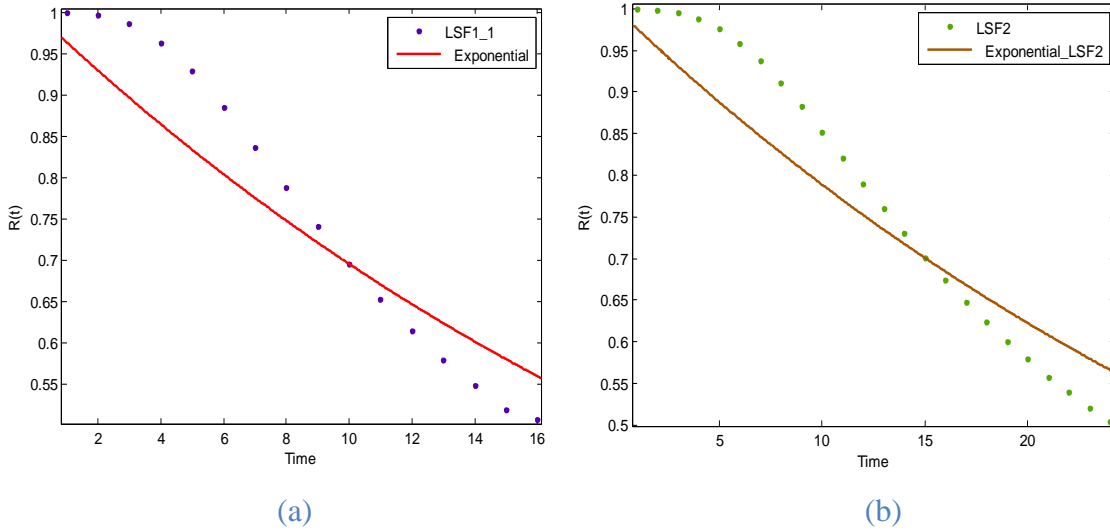


Figure 5:19: Curve fitting method to estimate the transition rate ϕ and λ

Estimation of repair rate ω for the case where repair and maintenance is performed may follow the repair rate model suggested by Fleming (2004) in Chapter 3 using the model given in Eq. (3.58):

$$\omega = \frac{P_I P_{FD}}{T_I + T_R} \quad (3.58)$$

where

P_I = the probability that piping element with a flaw will be inspected per inspection interval. The value will be 1 if it is in the inspection program or else it will be 0 (Vinod et al., 2003).

P_{FD} = the probability that a flaw will be detected given this element is inspected. This parameter is related to the reliability of Non Destructive Examination (NDE) inspection which is often referred to as Probability of Detection. For most NDE, its values are between 0.84 and 0.95 (Vinod et al., 2003).

T_I = the mean time between inspections for defects (For piping system, the inspection interval proposed by API 570 is either 5 or 10 years depending on the piping class. Refer to Table 3.1)

T_R = the mean time to repair once detected.

Using this equation, this study also attempted to estimate the repair rate using the values shown in Table 5.22. Monte Carlo simulation was used to generate the result and it gave $\omega = 0.044$ repair per year (mean time to repair was 22.7 years). This value was unreasonable and it did not make sense to have a very, very long repair time.

Table 5.22: Values used to determine the repair rate

Repair Rate Parameter	Values
Probability that a pipe element with flaw will be inspected per inspection interval (P_I)	1
Probability that an existing with flaw will be detected; probability of detection (P_{FD})	Between 0.84 to 0.94
Mean time between inspections for flaws; inspection interval, in years (T_{FI})	10
Mean time to repair the pipe element once flaw is detected, in days (T_R)	14

To validate the repair rate model, the actual repair time data was collected and the data was fitted to exponential distribution to in order to estimate the repair rate as shown in Figure 5.20. The result showed that the mean time to repair was 113 days (0.310 year) and converting the value to repair rate yields 3.23 repairs per year. Thus, this value will be used as the repair rate in this analysis.

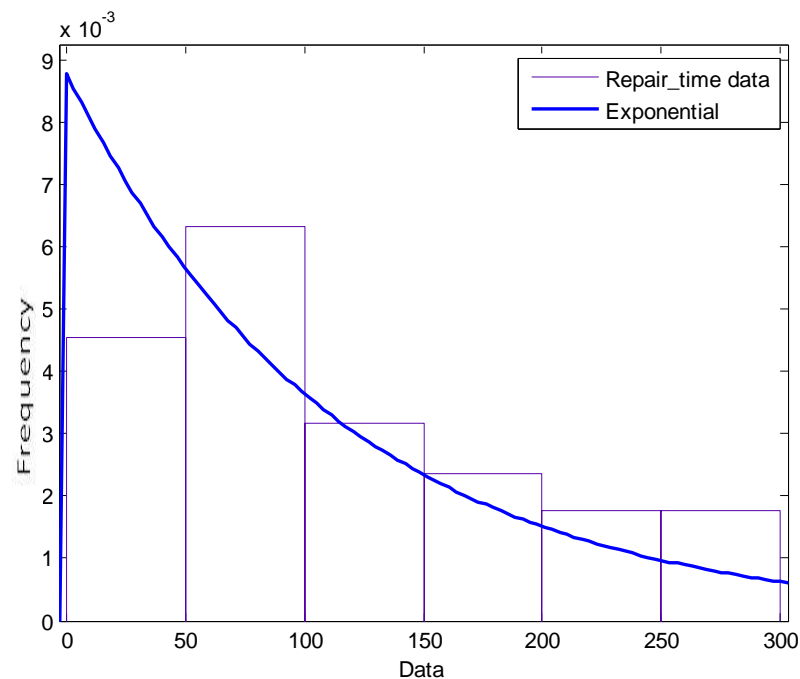


Figure 5.20: Distribution fitting for repair rate data

By putting the above-mentioned transition rates into the solved differential equation, the failure probabilities were generated as shown in Figure 5.21.

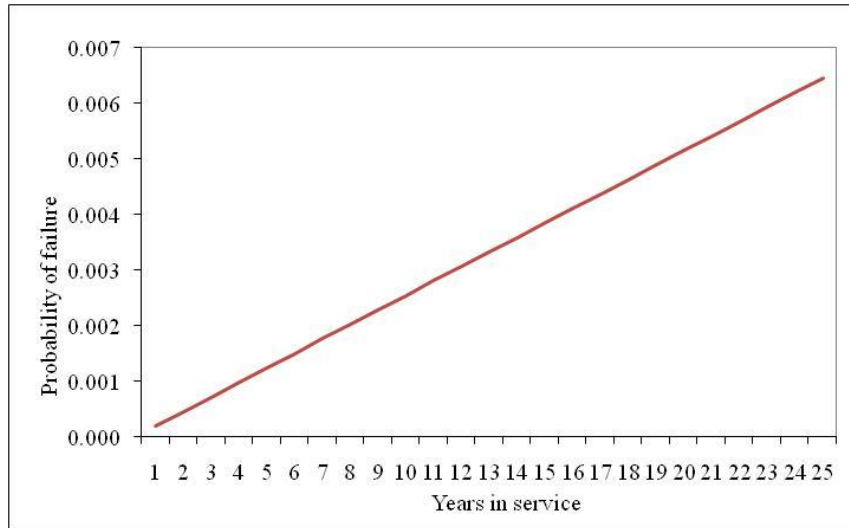


Figure 5.21: Probability of failure generated by the 3-state Markov model

5.4.3 Sensitivity analysis

5.4.3.1 The influence of corrosion rate

Estimation of corrosion rate is so critical and important in this analysis. For example, the following analysis for two different corrosion rate showed that there was a big different for the failure probability values produced as using the transition rates shown in Table 5.23. A 10-year inspection interval was used. Figure 5.22 shows the graph of the failure probability and it shows a strong relationship between the corrosion rate and the probability of failure.

Table 5.23: Influence of corrosion rate values on the failure probability values

Corrosion rate (mm/yr)	No repair		With repair	
	0.06	0.10	0.06	0.10
ϕ	0.0363	0.0610	0.0363	0.0610
λ	0.0237	0.0376	0.0237	0.0376
ω	0	0	3.23	3.23

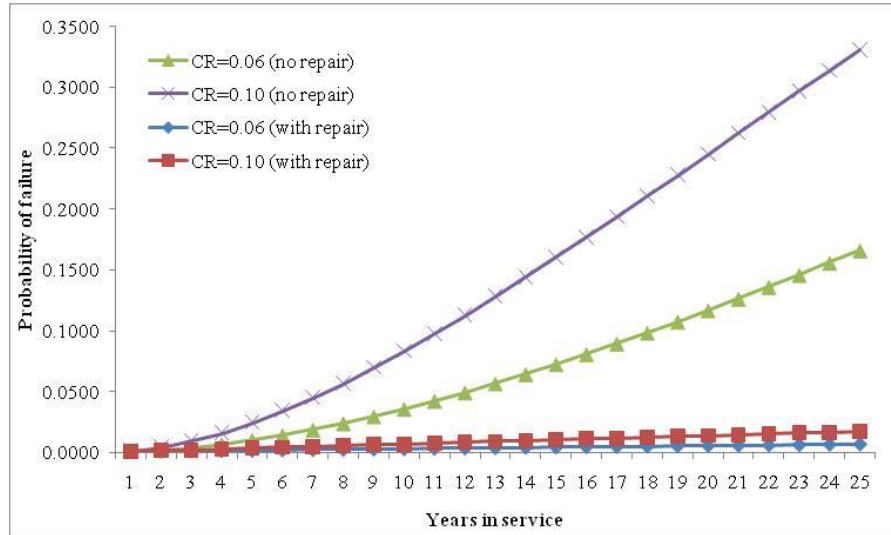


Figure 5.22: Influence of corrosion rate values on the failure probability values

5.4.3.2 The influence of different definition for each state

The definition for each state also investigated in this study. For example, the limit state function used to determine the transition rate ϕ from State 1 to State 2 is

$$g(x) = t_1 - (0.125t_{nominal} + CR \times T)$$

where the undetectable defect depth was assumed to be 0.125 of the nominal thickness $t_{nominal}$. An analysis was made to by assuming several cases such as

1. Undetectable defect depth is negligible.
2. Undetectable defect depth was assumed to be 0.05 of the nominal thickness, $t_{nominal}$.
3. Undetectable defect depth was assumed to be 0.10 of the nominal thickness, $t_{nominal}$.

4. Undetectable defect depth was assumed to be 0.125 of the nominal thickness, $t_{nominal}$.

The sensitivity analysis showed that definition of the state played an important role since the probability value produced will increase gradually as shown in Figure 5.23.

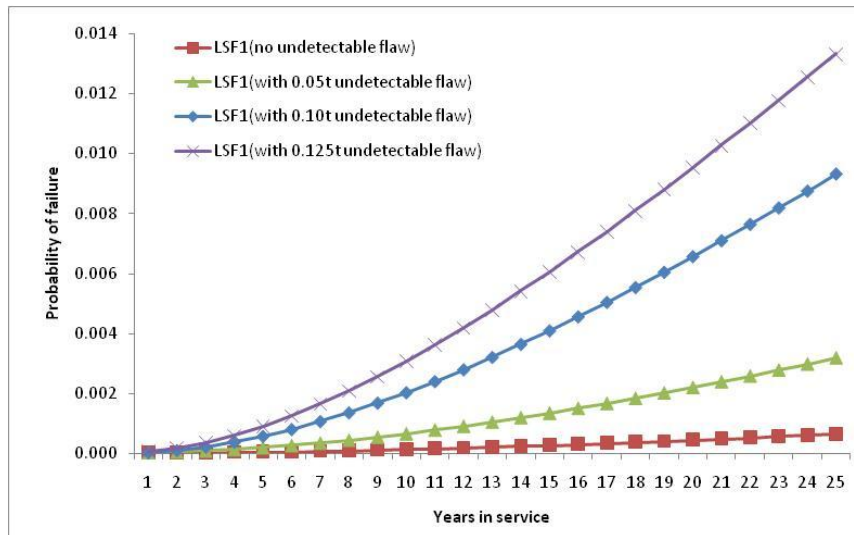


Figure 5.23: Effects of the failure probabilities to the different definition of State 1

5.4.3.3 The influence of different number of states

Prior study by Fleming (2004) suggested a three-state Markov model for thinning mechanism experienced by piping systems. However, what will be the impact if the number of states is more than 3? To understand the impact, this study compared the three-state Markov model with the four-state Markov model, also proposed by Fleming (2004) for all failure mechanisms. Table 5.24 shows the hypothetical definitions used to study the sensitivity of having the different number of states in generating the failure probability values; however, the last state, State 4 is also defined as when the wall thickness reaches the minimum wall thickness specified. Figure 5.24 illustrates the depth of corrosion. The same methodology was followed to determine the transition rates; however, MATLAB was used to solve the four-state Markov model.

Table 5.24: Description for the 4-state Markov model

State	Definition
1	d less than t_1
2	d is between t_1 and t_2
3	d is between t_2 and t_3
4	d is more than t_3

Note: d is the depth of corrosion, $t_1 = \frac{t_3}{3}$, $t_2 = 2t_1$, $t_3 = t_{nominal} - t_{minimum}$

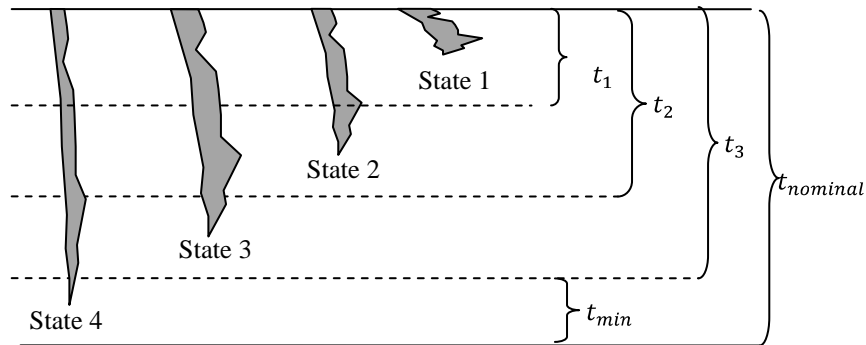


Figure 5.24: Illustration of the limit-state functions for 4-state Markov model

Based on Figure 5.25, it showed that the failure probability is sensitive to the number of states for Markov model where the three-state Markov model generates higher probability of failure when compared to the four-state Markov model.

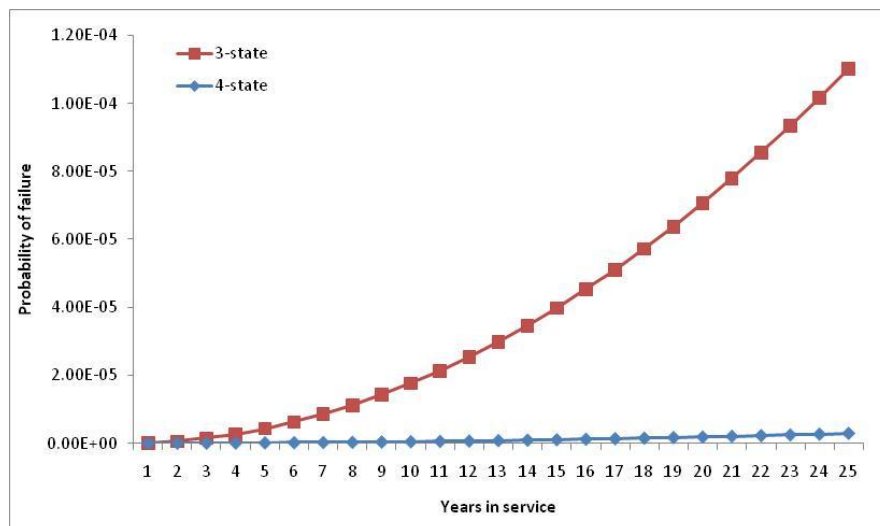


Figure 5.25: Effects of the failure probability to the different number of states (3- vs. 4-state)

5.4.4 Discussions

It has been demonstrated that the proposed three-state Markov model can be used as a tool to estimate the failure probability for piping systems subject to CUI. Also, the model can incorporate the impact of alternative strategies for inspection and leak detection. The main results of this model is that the failure probability is sensitive to the definition of states, the number of states as well as the corrosion rate used to calculate the transition rates.

The Markov model has demonstrated to be a useful tool to study the impact of alternative strategies for in-service inspection and leak detection. Together with appropriate estimation of its input parameters, the model is capable of making reasonable predictions of time dependent piping system reliability.

5.5 Concluding Remarks

Let one compare the four models explored in this study as shown in Table 5.25, Table 5.26 and Figure 5.26. Using logistic regression, one can see that the probability of having CUI if one opens the insulation at 15 years after pipe installation is 0.701 means that there is a 70.1% chances to have CUI if the insulation is removed. If one wait and do nothing to the pipe, the probability 0.962 which 96.2% chances of seeing CUI at year 25.

Degradation analysis shows that no failure can occur before 16 years ($\gamma = 15.59$), so the time scale starts at 16 years, and not 0. After year 16 years, the failure probability will increase following the Weibull 2-parameter distribution with $\beta = 1.729$ and $\eta = 38.157$ where the time-to-failure data were found fitted well in this distribution.

The failure probabilities at year 15 are close to zero which is 8.97×10^{-4} and 3.83×10^{-3} generated by the structural reliability analysis and continuous-time Markov model, respectively. However, for year 25, the structural reliability analysis gives the

highest probability value which is 0.280 comparing with 0.1514 (degradation analysis) and 6.43×10^{-3} (continuous-time Markov model). In other words, as time increase, the differences among these three models are very significant. This is expected as the underlying assumptions for these three models are different.

- Degradation analysis assumes the pipe will be at one of the two binary states (0 = failure and 1 = no failure). Failure here is defined as the time the wall thickness reached the minimum wall thickness specified. The degradation model used to extrapolate state 0 (i.e. the time-to-failure) employed different corrosion rate at each TMLs.
- The calculation of the structural reliability analysis is based in the concept of the difference between load and strength (or the boundary between desired and undesired performance of a pipe). In this case, a mode of pipe failure was when the pipe operating pressure or load exceeds the pipe failure pressure or capacity. In other words, at time t , how much the pipe with corrosion defect can withstand the same pressure inside the pipe?
- The results from the Markov model are the lowest. The main assumption for Markov model is that the pipe undergoes several states before the actual failure occur (failure is also defined as the wall thickness reached the minimum wall thickness specified). The transition rate from State 1 to State 2 is 0.0363/year and from State 2 to State 3 is 0.0237/year. In other words, the mean time the pipe will reach State 2 and 3 are 27.5 years and 42.2 years, respectively. This result is in agreement with the conclusions made by Vinod et al. (2003) where the probability of failure generated by Markov model is very small.

Table 5.25: Comparison among the four models

Model	Year 15		Year 25	
	Probability of failure at year 15	Likelihood Category	Probability of failure at year 25	Likelihood Category
Logistic Regression	0.701 (70.1% chances to have CUI if the insulation is removed)	Cannot compare with API 581 likelihood category	0.962 (96.2% chances to have CUI if the insulation is removed)	Cannot compare with API 581 likelihood category
Degradation Analysis (Weibull 3-parameter)	Zero	Very low	0.1514	Very High
Structural Reliability Analysis	8.97×10^{-4}	Very high	0.280	Very high
Continuous-Time Markov Model	3.83×10^{-3}	Very high	6.43×10^{-3}	Very high

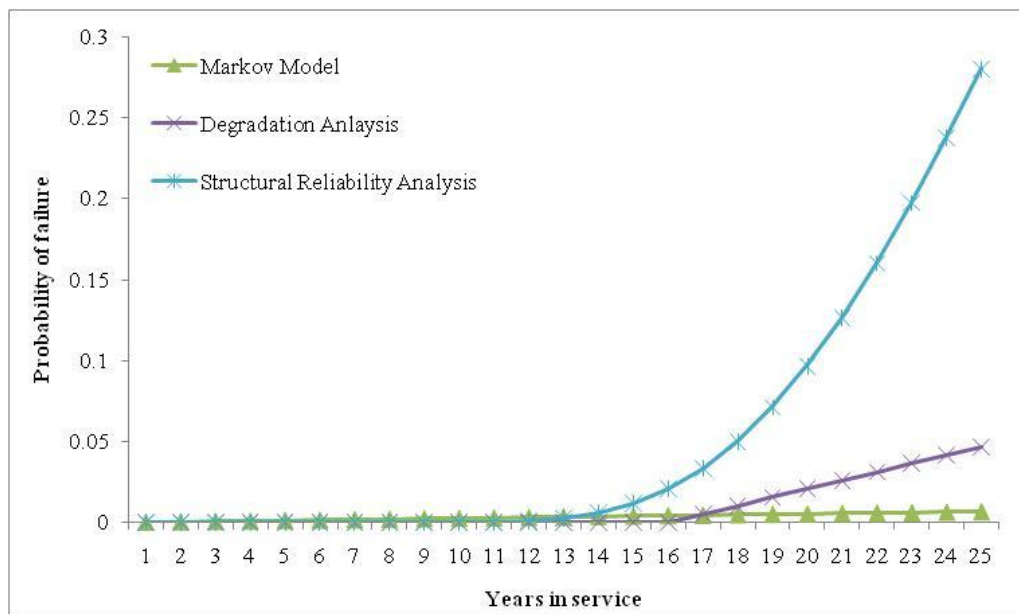


Figure 5.26: Comparison among the three proposed models

Table 5.26: Data required, findings and recommendation for each model

Model	Data required	Findings	Recommendations
Logistic regression model	Internal visual inspection data (binary data, i.e. CUI found = 1 or CUI is not found = 0)	<ul style="list-style-type: none"> Produced a mathematical model that provides the likelihood of having CUI for piping systems given the pipe age, operating temperature and insulation type. Proved the research hypothesis which is small bore pipes will give higher tendency to experience CUI when compared to big bore pipes. 	To include other factors that contribute to CUI such as humidity (i.e. marine, temperate, dry), pipe complexity (i.e. number of branches), etc. in the mathematical model.
Degradation analysis	<ul style="list-style-type: none"> Initial/nominal and minimum wall thickness Wall thickness data: to estimate the corrosion rate; to extrapolate the time-to-failure 	<ul style="list-style-type: none"> The time-to-failure data for CUI which is based on a linear degradation model obeys either the lognormal or Weibull distributions which were not known before. Based on the Weibull distribution, the shape parameter β for very cold or very hot piping systems (operating temperature $< -12^{\circ}\text{C}$ or $> 121^{\circ}\text{C}$, respectively) is less than 1 which indicates that the failure rate decreases over time. Up to a point, the failure rate will become constant (i.e. failure rate = 1). Planned inspection/maintenance has no advantage in these cases because failure will occur at random. For piping systems that operate between -12°C and 121°C, the shape parameter β is more than 1 which implies that the failure rate increases over time. The increasing failure rate indicates wear out such as corrosion and such pipes will have higher risk of failure. The main obstacle with this method is to have enough data to establish the statistical distribution; else prediction using this method is not viable. If plant people were to adopt this method, then more wall thickness measurements have to be collected at more TML along a specified pipe which may increase the cost of opening the insulation and reinsulated the pipe back or the cost of using suitable NDT techniques without opening the insulation. 	<ul style="list-style-type: none"> To have more TML for pipe within the operating temperature susceptible to CUI. Frequent inspection interval is recommended for piping systems with failure rate more than 1 (i.e. failure rate increases over time).
Structural reliability analysis	<ul style="list-style-type: none"> Wall thickness data: to estimate the corrosion rate Design data: material yield strength, pipe diameter, pipe thickness 	<ul style="list-style-type: none"> Both the thinning model and the modified B31G predicted similar values of the failure probabilities. FORM and Monte Carlo simulation reliability algorithms produce similar results when the limit state function can be linearized and the load and resistance variables have normal probabilistic distributions. In 	<ul style="list-style-type: none"> The probabilistic analysis of a pipe must be performed independently for deep and shallow defects in order to ensure a correct repair strategy

	<ul style="list-style-type: none"> Operating data: operating pressure 	<p>this case, with 10,000 runs, it is already reaching the convergence.</p> <ul style="list-style-type: none"> The pipe failure probability increases with increased service life and that the rate of change of pipe failure probability also increases gradually with the increase service life. At low service life (about 10 to 12 years in service), <ul style="list-style-type: none"> the pipe reliability is almost insensitive to the input variables but the sensitivity of the failure probability estimate increases gradually with increased service life. the pipe reliability is almost insensitive to COV of the load and resistance variables. However, special care must be taken in characterizing accurately COV of the variables if the reliability of pipes is assessed for longer years in service. Moreover, it is pointed out that if the reduction in pipe safety is assessed for long service times, then special care must be taken in charactering COV of the variables (1) corrosion rate, (2) pipe wall thickness (in that order). At any service life, the pipe reliability is almost insensitive to pipe diameter, material strength and pipe operating pressure. It is observed that the pipe falling under very high category indicating the most significant pipe needs to be investigated through RBI. Numerical simulations have been performed and allow describing the evolution of the safety index of the insulated pipes with time. 	<p>for shorter and longer years in service.</p> <ul style="list-style-type: none"> If the probabilistic distribution of a load and resistance is not experimentally available, the sensitivity of the pipe reliability to this variable is the key to assume its distribution type. The last important point is the interest to better estimate the coefficient of variation associated to corrosion rate because it is a parameter of great influence towards numerical simulations. The graph, reliability index versus years in service would be a good guide to set the effective remaining service life. After this period, even if it appears that the pipe has not failed, it would not be safe to use it. For reasons of safety, it would be wise for the pipe to be repaired or replaced, in order to decrease its failure probability if further service is required of it. This graph will be used to plan effective and economic inspection, repair and replacement programs.
Continuous time Markov model	<ul style="list-style-type: none"> Wall thickness data: to estimate the corrosion rate Design data: material yield 	<ul style="list-style-type: none"> Typically, actual wall thickness data is used to estimate the transition rates. However, the data was not enough to do so. Thus, the structural reliability analysis (i.e. FORM model) was used to estimate the 	<ul style="list-style-type: none"> If plant people were to adopt Markov model, then the following needs to be done:

	<p>strength, pipe diameter, pipe thickness</p> <ul style="list-style-type: none"> • Operating data: operating pressure 	<p>transition rate and it is found that the prediction using this method is viable. Taking the wall thickness data periodically will increase the cost of opening the insulation and reinsulated the pipe back.</p> <ul style="list-style-type: none"> • The number of states was an important parameter since the generated probability of failure by the 3-state and 4-state Markov model were statistically significant. • The definition of states also was an important factor since the generated probability of failure by the difference definition of state was statistically significant. 	<ul style="list-style-type: none"> • To determine the correct number of states. • To determine the suitable definition for each state.
--	---	---	--

